Available online at www.sciencedirect.com
SCIENCE DIRECT
Geochimica et Cosmochimica Acta 70 (2006) 839–857
Geochimica
www.elsevier.com/locate/gca

Interaction between zinc and freshwater and marine diatom species: Surface complexation and Zn isotope fractionation

A. Gélabert [a], O.S. Pokrovsky [a,*], J. Viers [a], J. Schott [a], A. Boudou [b], A. Feurtet-Mazel [b]

[a] *Laboratoire de Mécanismes et Transfert en Géologie (LMTG), UMR CNRS 5563, Université Paul Sabatier, 14 Avenue Edouard Belin, 31400 Toulouse, France*
[b] *Laboratoire d'Ecotoxicologie et d'Ecophysiologie des Systèmes Aquatiques (LEESA), UMR CNRS 5805, Université de Bordeaux 1, Place du Dr Peyneau, 33120 Arcachon, France*

Received 18 May 2005; accepted in revised form 24 October 2005

Abstract

This work is devoted to characterization of zinc interaction in aqueous solution with two marine planktonic (*Thalassiosira weissflogii* = TW, *Skeletonema costatum* = SC) and two freshwater periphytic species (*Achnanthidium minutissimum* = AMIN, *Navicula minima* = NMIN) by combining adsorption and electrophoretic measurements with surface complexation modeling and by assessing Zn isotopes fractionation during both long term uptake and short term adsorption on diatom cells and their frustules. Reversible adsorption experiments were performed at 25 and 5 °C as a function of exposure time (5 min to 140 h), pH (2 to 10), zinc concentration in solution (10 nM to 1 mM), ionic strength ($I = 0.001$ to 1.0 M) and the presence of light. While the shape of pH-dependent adsorption edge is almost the same for all four species, the constant-pH adsorption isotherm and maximal Zn binding capacities differ by an order of magnitude. The extent of adsorption increases with temperature from 5 to 25 °C and does not depend on light intensity. Zinc adsorption decreases with increase of ionic strength suggesting competition with sodium for surface sites. Cell number-normalized concentrations of sorbed zinc on whole cells and their silica frustules demonstrated only weak contribution of the latter (10–20%) to overall zinc binding by diatom cell wall. Measurements of electrophoretic mobilities (μ) revealed negative diatoms surface potential in the full range of zinc concentrations investigated (0.15–760 μmol/L), however, the absolute value of μ decreases at [Zn] > 15 μmol/L suggesting a change in surface speciation. These observations allowed us to construct a surface complexation model for Zn binding by diatom surfaces that postulates the constant capacitance of the electric double layer and considers Zn complexation with carboxylate and silanol groups. Thermodynamic and structural parameters of this model are based on previous acid–base titration and spectroscopic results and allow quantitative reproduction of all adsorption experiments. Although Zn adsorption constants on carboxylate groups are almost the same, Zn surface adsorption capacities are very different among diatom species which is related to the systematic differences in their cell wall composition and thickness. Measurements of Zn isotopic composition ($^{66}Zn/(^{64}Zn)$) performed using a multicollector ICP MS demonstrated that irreversible incorporation of Zn in cultured diatom cells produces enrichment in heavy isotope compared to growth media ($\Delta^{66}Zn$(solid–solution) = 0.27 ± 0.05, 0.08 ± 0.05, 0.21 ± 0.05, and 0.19 ± 0.05‰ for TW, SC, NMIN, and AMIN species, respectively). Accordingly, an enrichment of cells in heavy isotopes ($\Delta^{66}Zn$(solid–solution) = 0.43 ± 0.1 and 0.27 ± 0.1‰ for NMIN and AMIN, respectively) is observed following short-term Zn sorption on freshwater cells in nutrient media at pH ~ 7.8. Finally, diatoms frustules are enriched in heavy isotopes compared to solution during Zn adsorption on silica shells at pH ~ 5.5 ($\Delta^{66}Zn$(solid–solution) = 0.35 ± 0.10‰). Measured isotopes fractionation can be related to the structure and stability of Zn complexes formed and they provide a firm basis for using Zn isotopes for biogeochemical tracing.

1. Introduction

Diatoms, unicellular brown algae enclosed in an external siliceous skeleton (frustule), account for a quarter of all the photosynthesis on the planet. As their cell wall is

* Corresponding author. Fax: +33 5 61 33 26 50.
E-mail address: oleg@lmtg.obs-mip.fr (O.S. Pokrovsky).

0016-7037/$ - see front matter © 2005 Elsevier Inc. All rights reserved.
doi:10.1016/j.gca.2005.10.026

known to display a high affinity for a wide range of aqueous metal cations, they are able to play a key role in metal speciation and distribution in many aquatic systems as well as in trophic transfer capacities to the benthic and pelagic foodwebs. As a result, diatoms are considered as bioindicators of water pollution in rivers (Dixit et al., 1992; Gold et al., 2003a,b) or in sewage sludge (Pun et al., 1995) and are widely used as metal removal agent (Volesky and Holan, 1995; Csogor et al., 1999; Vrieling et al., 2000; Schmitt et al., 2001). Many studies have been devoted to metal uptake and adsorption by marine planctonic diatoms (Rijstenbil et al., 1994; Gonzalez-Davila, 1995; Gonzales-Davila et al., 2000; Wang and Dei, 2001a,b; Rijstenbil and Gerringa, 2002), diatom response to metal stress (Fisher and Fabris, 1982; Ahner et al., 1997; Sunda and Huntsman, 1998) and their growth limitation by trace elements (Anderson et al., 1978; Brand et al., 1986; Morel et al., 1991; Ivorra et al., 2000). At the same time, freshwater diatoms received relatively little attention despite their importance in metals regulation in continental waters (Gold et al., 2002; Tien, 2004) owing to their accumulation and transfer capacities along the foodwebs (Genter, 1996).

Among metals, zinc is of great interest because it is considered both as an essential micronutrient at low concentration (Morel et al., 1991, 1994) and as a toxic element at high concentration (50–200 mg/L) leading to depressed division rates or growth inhibition (Jensen et al., 1974, 1982; Fisher et al., 1981, 1986). Inside the cell, zinc constitutes the major pool of metal ions and is usually associated with numerous proteins and enzymes (Vallee and Auld, 1990) but is also stored in carboxylate or polyphosphate complexes (Stauber and Florence, 1990; Kotrba et al., 1999; Cox et al., 2000; Frausto da Silva and Williams, 2001). Again, most of available information on zinc deals with marine diatom species due to their importance in Zn regulation in seawater (Sunda and Huntsman, 1992) and their potential use as proxies (Elwood and Hunter, 1999), and leave apart freshwater species. This study is aimed at filling this gap by providing a quantitative comparison of zinc binding to two marine planctonic and two freshwater periphytic species.

It has been widely argued that molecular mechanisms operating at solid–solution interface are likely to be responsible for isotopic fractionation of "heavy" elements (Johnson et al., 2004). For example, isotopic fractionation of Zn (Cacaly et al., 2004; Rouseset et al., 2004; Pokrovsky et al., 2005b), Ge (Galy et al., 2002) and Mo (Barling and Anbar, 2004) has been reported during these elements adsorption on solid oxy(hydr)oxides. The role of biota in Zn isotopic fractionation in oceanic sediments (Pichat et al., 2003) as well as in its terrestrial cycle (Viers et al., 2004) has been largely evoked, however, to our knowledge, there is no experimental study of Zn isotopic fractionation during its uptake or adsorption by microorganisms.

Because the first step in metal uptake process by biota is aqueous ions or complexes adsorption on external cell layers (cell wall, plasmic membrane), studying this "primary" adsorption process is crucial for modeling the impact of aquatic organisms on metal transport in natural settings. The aim of this study, therefore, is to provide, within the framework of chemical equilibrium, a description of diatoms interactions with zinc by combining macroscopic adsorption and electrokinetic measurements with surface complexation modeling. Complementary to this, $^{64}Zn/^{66}Zn$ isotopes fractionation during viable cells and frustules adsorption experiments as well as long term uptake were performed to assess the main factors controlling isotope fractionation and possibility to use this fractionation for tracing geochemical processes. In this work we retained four representative diatom species which are very abundant in temperate climate zone: two planktonic, *Skeletonema costatum* (marine) and *Thalassiosira weissflogii* (estuarine) and two freshwater periphytic, *Achnathidium minutissimum* and *Navicula minima*.

In the first part of this study it was demonstrated that the four diatom species have a similar cell wall structure which is mainly composed of polysaccharides and proteins coating the silica frustule (Gélabert et al., 2004). The main surface moieties of this complex 3D-cell wall structure are amino, carboxyl and silanol groups that control both surface charge, and, presumably, affinity to metal ions. Since diatoms site densities normalized to the area of siliceous shell are an order of magnitude higher than corresponding values for organic-free frustules, the metal affinity of diatom cultures is expected to be essentially controlled by the 3D organic layer covering the silica frustule.

In the present study we are trying to address the following issues: (i) what are the main "external" (environmental) parameters controlling the interaction of zinc with diatom surfaces? (ii) what are the differences in zinc binding properties between freshwater and marine species? (iii) what are the main functional groups responsible for Zn sorption on diatom surfaces, and (iv) is it possible to relate the isotopic fractionation produced by Zn interaction with diatom cultures to the structure and stability of metal complexes formed? We hope that answering these questions will provide a firm basis for quantitative biogeochemical modeling of zinc transport in natural environments controlled by aquatic biological communities.

2. Material and methods

2.1. Diatom cultures

Monospecific diatom cultures were developed from laboratory strains to separately produce biomass of four species: marine planctonic *T. weissflogii* (abbreviated TW), *S. costatum* (SC), freshwater periphytic *A. minutissimum* (AMIN) and *N. minima* (NMIN) as described previously (Gélabert et al., 2004). Diatoms were cultured to concentration of $\sim 10^7$ cell/L at 20 °C in a sterile Dauta (freshwater) or f/2 (seawater) medium (Gold et al., 2003a) at pH $\sim$ 7.7–7.8 and $[Zn]_{tot} \sim 0.2$ μM. Continuous aeration of the culture was provided to prevent pH from increasing

due to photosynthetic activity. Typical incubation time was 1–2 weeks. Diatoms were harvested from the late exponential—stationary growth phase and kept at 4 °C until use.

The biomass of live diatom cells suspension was quantified by its humid (centrifuged 15 min at 2200*g*) and dry (lyophylized) weight. Before the adsorption experiment, diatoms were rinsed three times in appropriate NaCl or $NaNO_3$ solution using centrifugation at 2200*g* (~400 mL of solution for 1 g of wet biomass) to remove the adsorbed metals and cell excudates from the surface. Diatom frustules were extracted from cells suspension (20 g humid/L) by acid digestion (5% HNO_3 + 5% H_2O_2) during 6 h at 105 °C followed by thorough rinsing in sterile deionized water using centrifugation. FT-IR, XRD and SEM analysis of produced solid material revealed only amorphous silica ($SiO_2 \cdot nH_2O$) without detectable traces of organic constituents.

2.2. Zinc adsorption experiments

Zinc adsorption experiments were designed to provide a quantitative characterization of Zn binding by diatom surface via determining thermodynamic stability constant for adsorption reaction on different surface sites. For this, two types of experiments were performed: (i) adsorption at constant initial zinc concentration in solution as a function of pH (pH-dependent adsorption edge) and (ii) adsorption at constant pH as a function of zinc concentration in solution (''Langmurian'' isotherm). Furthermore, the influence of other environmental parameters such as ionic strength, biomass concentration, light intensity, temperature and time of exposure were also investigated. All experiments were performed in solutions undersaturated with respect to any solid metal oxide, hydroxide or carbonate phase as verified by calculation using MINTEQA2 computer code and corresponding database (Allison et al., 1991).

Adsorption experiments were conducted at 25 ± 0.2 °C in continuously stirred diatom suspension of $NaNO_3$ or NaCl solution with ionic strength ranging from 0.001 to 1 M using 8 mL sterile polypropylene vials. Cell concentrations varied from 8 to 70 g humid/L ($(2–4) \times 10^9$ cells/L) and zinc concentration in solution ($[Zn]_{aq}$) spanned from 0.7 to 800 μM. pH was adjusted to the desired value using either NaOH or HNO_3 (HCl for NaCl electrolyte). HEPES buffer, which is known to do not complex divalent metals in aqueous solutions (Mirimanoff and Wilkinson, 2000), was added to a concentration of 0.003 M in order to keep pH constant during adsorption isotherm measurements. For all experiments, sterile de-ionized water (MilliQ, 18 mΩ) purged of CO_2 by N_2 bubbling was used. At the end of the experiment, the suspension was centrifuged and the resulting supernatant filtered through a 0.22 μm Nylon filter, acidified with ultrapure nitric acid and stored in the refrigerator until analysis. The concentration of metal adsorbed to diatom in each vessel were calculated by substracting the concentration of metal in the supernatant from the original amount of zinc added in the suspension. To account for Zn adsorption on reactor's walls, supernatants obtained from diatom suspensions were conditioned at $4 \leqslant pH \leqslant 8.5$ and the same concentration of added Zn as in cell adsorption experiments. After 3 h, no significant decrease of initial Zn concentration was detected upon filtration indicating on the absence of Zn adsorption on the reactor walls and Zn hydroxide formation in solutions. Only at $pH > 8.5$ and $[Zn]_t \geqslant 10^{-4}$ M, a ~30% decrease of Zn concentration in blank experiments was observed. This was taken into account when calculating the net adsorption yield.

Exposure time varied intentionally from 15 min to 140 h to assess the influence of kinetics on Zn sorption. For most of experiments, exposure time was fixed to 3 h. Optical microscopic inspection of diatoms before and after adsorption experiments showed no visible change in the diatoms population. The cells and chloroplasts remained intact and non-deformed, and no cell fragments could be detected.

2.3. Electrophoretic measurements

These experiments were designed to assess the cell surface potential or zeta-potential, and, by monitoring its dependence on Zn concentration in solution, to better constrain the surface complexation reactions (see Section 3.3 below). This method allows very fast, in situ estimation of the sign of electric surface potential and monitoring of its qualitative modification in the course of metal adsorption. Electrophoretic mobilities of live diatom cells *A. minutissimum* and *T. weissflogii* were measured at 25 °C using a microelectrophoremeter (''Zetaphoremeter IV'' Z4000, CAD Instrumentation). Details are given in Gélabert et al. (2004). Three replicates were carried out and each replicate was performed by renewing the suspension in the microelectrophoresis cell. The uncertainty attached to electrophoretic mobilities were less than 5%. Experiments were performed with viable cells (~1 g humid/L) under constant ionic strength (0.01 and 0.1 M) in solutions with zinc concentration ranging from 0.15 to 800 μM and pH around 7. All solutions were undersaturated with respect to solid oxides and hydroxides of zinc. The time of cells exposure to Zn-bearing solutions varied from 5–10 min to 3 h.

2.4. Analytical methods

All filtered solutions were analyzed for Zn ($[Zn]_{aq}$) using flame atomic absorption (Perkin Elmer 5100 PC spectrophotometer) with an uncertainty of ±1% and a detection limit of 10^{-7} g/L. For Zn concentration lower than 100 μg/L, analyses were performed by ICP-MS on Perkin Elmer SCIEX, Elan 6000 with a detection limit of 0.01 μg/L and a precision of ±5%. Values of pH were measured using a Mettler Toledo combined electrode, with an accuracy of ±0.002 units. Dissolved organic carbon (DOC)

was analyzed using a Carbon Total Analyzer (Shimadzu TOC-5000) with an uncertainty of 3% and a detection limit of 0.1 ppm.

2.5. Zn stable isotope measurements

Three types of experiments have been performed to study zinc stable isotope fractionation during its interaction with diatom cultures: (i) long-term Zn uptake (incorporation) in Dauta media in batch growing cultures (AMIN, NMIN, TW, SC) during 3–4 weeks with periodical renewing of nutrient solution to provide a semi-constant zinc concentration at 0.30 ± 0.05 μM; (ii) short-term interaction of Zn with viable diatom cultures AMIN and NMIN in nutrient media; and (iii) reversible adsorption of Zn on NMIN frustules as a function of pH in 0.01 M $NaNO_3$. For the uptake experiments (1), both the initial solution and growing biomass were analyzed while for the adsorption experiments (2) and (3), only filtered solution was processed.

Diatom cells harvested by centrifugation at 2500*g* were dried at 80 °C and grounded using agate mortar and pestle. Hundred milligrams of this powder was submitted to hydrogen peroxide digestion (H_2O_2) followed by acid digestion (HNO_3 + HF) in a clean bench room. Blank tests were performed to estimate the level of Zn contamination induced by the digestion procedure and were found to be less than 0.2%. The International Geostandard SRM 1515 (Apple Leaves, from NIST, USA) was used to check the validity and the reproducibility of both the acid digestion and ICP-MS analyses. The relative difference between our values and the certified data was close to 5%.

In isotopic fractionation experiments, a full recovery of filtered solution during preparation procedure is crucial. Filtration of supernatant in (2) and (3) type experiments did not affected the fractionation coefficients because such a filtration of initial Zn stock solution did not change δ^{66}Zn within the uncertainty ($\pm 0.05‰$) as verified by: (i) ICP-MS-MC measurements on this filtered sample subjected to ion-column purification procedure, and (ii) a $100 \pm 1\%$ recovery of $[Zn]_{aq}$ in filtered standard solutions at pH 6–7 as measured by AAS.

Zn isotopic composition has been measured at Lyon (Ecole Normale Supérieure) on the P54 MC-ICP-MS (VG Elemental) and at Toulouse (LMTG) on the Neptune MC-ICP-MS (ThermoFinnigan). Zn has five stable isotopes of mass 64, 66, 67, 68, and 70 whose average abundances are 48.63, 27.90, 4.10, 18.75, and 0.62%, respectively. Zn was isolated from the bulk sample using the purification procedure of Maréchal et al. (1999) on the AGMP-1 anion exchange resin (Bio-Rad, USA). An aliquot containing about 300 ng of Zn was loaded on the column. Because isotopic fractionation may occur during the elemental separation on the ion-exchange resin (Maréchal and Albarède, 2002), we analyzed only the samples for which the separation procedure gave a yield of 100% taking into account the analytical uncertainties. The ^{62}Ni signal was simultaneously measured to evaluate the isobaric interference of ^{64}Ni on the ^{64}Zn signal; no significant interference was found. Instrumental mass fractionation was corrected following the method described by Maréchal et al. (1999). A Cu standard (NIST 976) was added to the purified Zn fractions and a Cu (NIST 976) + Zn (JMC 3-0749L) standard mixture was run as a bracketing standard. The ratio of Cu and Zn fractionation factors (i.e., f_{Cu}/f_{Zn}) was found to be constant over a single analytical session (i.e., one day measurement) for both P54 and Neptune instruments. As already observed by Maréchal et al. (1999) and Pichat et al. (2003) this f_{Cu}/f_{Zn} ratio does not remain constant from one day to another. The slope of the fractionation line derived from the standard mixture raw data in a $\ln(^{66}Zn/^{64}Zn)$ versus $\ln(^{65}Cu/^{63}Cu)$ plot was used to correct the data on the Zn sample + Cu standard mixtures. The Zn isotopic results in this study are given in the recommended delta notation for the ^{66}Zn/^{64}Zn ratio (Albarede, 2004):

$$\delta^{66}Zn = [(({}^{66}Zn/{}^{64}Zn)_s/({}^{66}Zn/{}^{64}Zn)_{JMC}) - 1] \times 1000 \text{ (in } ‰), \quad (1)$$

where s signifies sample and JMC the Zn isotopic standard solution. Note that this JMC 3-0749L solution is not a referenced material but an elemental standard solution used by several laboratories. The δ^{67}Zn and δ^{68}Zn were also considered to check the validity of the measurements and to check that the different Zn isotopes fit on a theoretical mass-dependent fractionation line. The uncertainty given for the δ^{66}Zn varies from 0.05 to 0.1‰.

For experiments (2) and (3) performed in a closed system, the isotopic signature of solid phase ($\delta^{66}Zn_{solid}$) was calculated from the mass balance equation using the isotopic ratio in aqueous phase ($\delta^{66}Zn_{aq}$), the amount of metal adsorbed (A, %), and the isotopic composition of initial solution ($\delta^{66}Zn_{initial}$):

$$\delta^{66}Zn_{solid} = \{100 \cdot \delta^{66}Zn_{initial} - (100 - A) \cdot \delta^{66}Zn_{aq}\}/A. \quad (2)$$

In this work, we define the isotopic offset between Zn in solution and Zn adsorbed or incorporated in diatoms cells and frustules as

$$\Delta^{66}Zn(\text{solid-solution}) = \delta^{66}Zn_{solid} - \delta^{66}Zn_{aq}. \quad (3)$$

For experiments (1) on cultures growing under constant concentration of zinc, the isotopic offset is determined as the difference between δ^{66}Zn in digested cells and that in the Zn salt used to prepare the growth media.

3. Experimental results

3.1. Adsorption

Measurements of zinc adsorption kinetics on diatom cells indicate that majority of zinc is sorbed within the first 10–100 min of exposure (Fig. 1), in agreement with

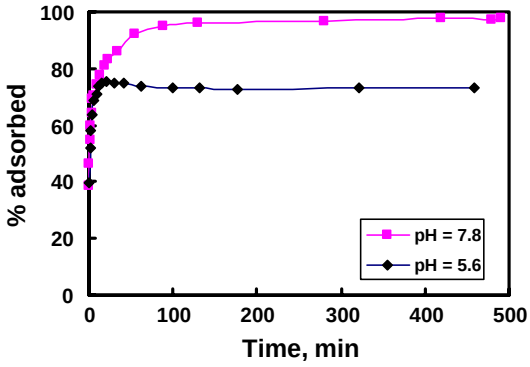

Fig. 1. Kinetics of zinc adsorption on *Navicula minima* species. Experimental conditions: 0.001 M $NaNO_3$; biomass concentration equals 8.5 g humid/L; $[Zn]_o = 61$ µmol/L; continuous shaking at 25 °C in the dark.

previous works on metal adsorption onto bacteria (Fein et al., 1997; Ngwenya et al., 2003) and algae (Xue et al., 1988; Gonzales-Davila et al., 1995, 2000).

The reversibility of Zn adsorption equilibria was first tested following the method developed by Fowle and Fein (2000). A homogeneous parent suspension solution of diatoms + Zn + electrolyte was adjusted to pH ~ 7 at which 100% Zn was adsorbed onto diatoms. After 3 h of adsorption contact time, aliquots of this parent suspension solution were taken and adjusted to sequentially lower pH values (2–6.9). The reaction vessels equilibrated at new pH values for 3 h were sampled for Zn (Fig. 2A). The concentration of "desorbed" zinc in the supernatant allowed calculation of the amount of irreversibly "incorporated" metal. This amount never exceeded 5–10% suggesting an equilibrium adsorption process with negligible amount of zinc penetrating inside the cell. The second method of reversibility test, developed in the present study, consists of preparing a series of reactors having the diatoms suspension with constant concentration of initially added zinc ($[Zn]_o$) in a wide pH range, separating the cells and the supernatant by centrifugation and filtration and measuring dissolved (<0.2 µm) zinc concentration in the first filtrate ($[Zn]_1$). Afterwards, for each investigated pH, exact amount of new zinc-free electrolyte solution is added to wet centrifuged biomass in each reactor and "desorbed" aqueous zinc concentration in the second filtrate ($[Zn]_{desorb}$) is monitored after 3 h of reaction. The proportion of irreversibly bound metal ($[Zn]_{incorp}$) is calculated as

$$[Zn]_{incorp}(\%) = 100 \cdot \{([Zn]_o - [Zn]_1 - [Zn]_{desorb})/[Zn]_o\}. \quad (4)$$

This method was tested for zinc adsorption by *S. costatum* species for which very good recovery of adsorbed zinc, meaning low amount of irreversibly bound zinc (i.e., 5–10%), was found (Fig. 2B).

Concentration of dissolved organic carbon in the course of adsorption experiment did not change by more than 30–50% as illustrated for two marine species in Fig. 3. Only weak degradation of cell wall in usual pH range of adsorption experiments ($4 \leqslant pH \leqslant 8$) was observed. Low DOC concentration monitored during adsorption experiments (i.e., 2–4 mg/L, comparable with [DOC] in surface seawa-

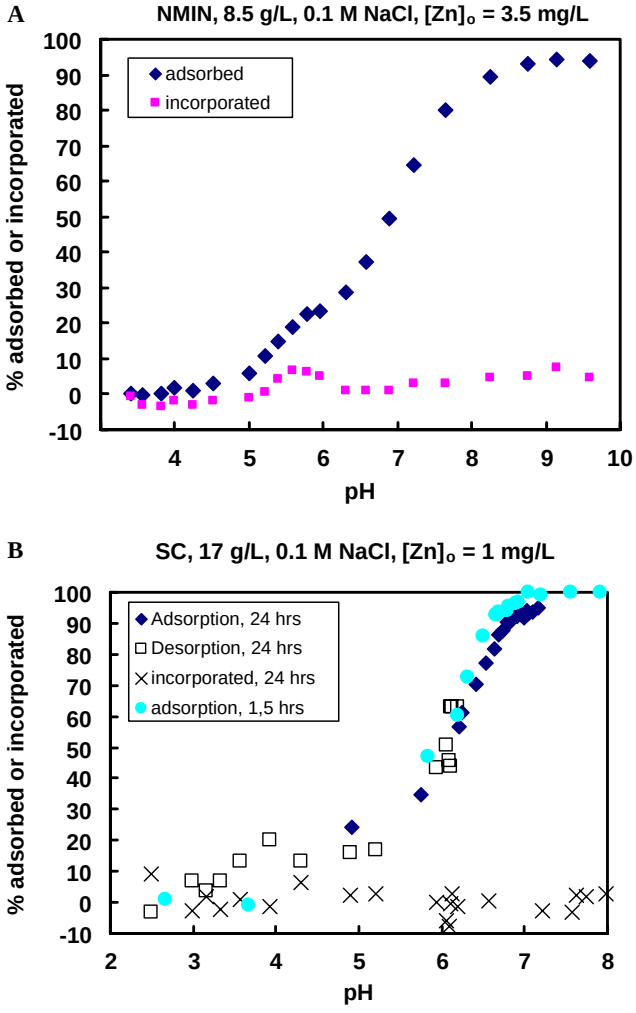

Fig. 2. Reversibility of adsorption equilibria: percentage of adsorbed or incorporated zinc as a function of pH for *Navicula minima* (A) and *Skeletonema costatum* (B).

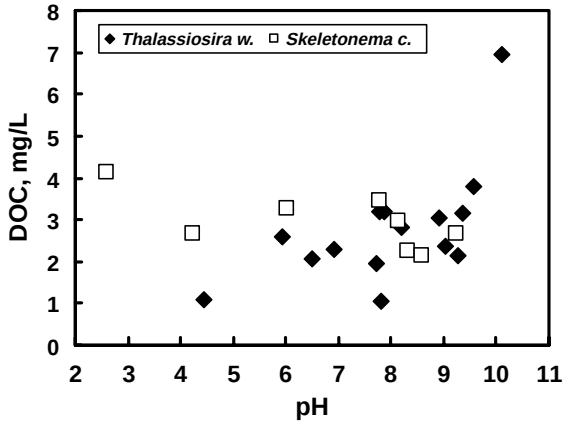

Fig. 3. Dissolved organic carbon (DOC) concentration as a function of pH during Zn adsorption experiments. Experimental conditions: biomass concentration equals 36 g/L (TW) and 8.5 g/L (SC); 0.1 M NaCl; $[Zn]_o = 51$ µmol/L. Exposure time equals 3 h in the dark.

ter) and relatively high Zn and cell biomass concentration (1.5–50 μM and 8–70 g/L, respectively) imply that diatom surface functional groups, and not organic exudates, are primary responsible for Zn binding in studied systems.

Full compilation of adsorption experiments is given in the Electronic annex and summarized in Table 1. Altogether, ~50 experiments having 15–30 data points each have been performed for 4 species and their frustules. Results of zinc adsorption experiments on diatoms as a function of pH and zinc aqueous concentration are depicted in Figs. 4–9. For each species the general trend is a negligible adsorption of zinc at pH < 4–5, strong increase in adsorp-

Table 1
Summary of adsorption experiments

Exp. No	Species	Number of data points	Cell conc. (g humid/L)	$[Zn]_o$ (μmol/L)	pH	Electrolyte
Langmurian adsorption isotherm						
36	SC	14	8.5	0–61	7.50 ± 0.02	0.1 M $NaNO_3$
47	SC	20	8.5	0–184	7.15 ± 0.02	0.1 M NaCl
103	SC	40	8.5	0–444	7.2 ± 0.1	0.01 M NaCl
107	SC	27	36	0–735	7.3 ± 0.1	0.1 M NaCl
70	TW	32	35	0–168	7.60 ± 0.01	0.1 M NaCl
33	AMIN	10	8.6	0–41	9.2 ± 0.6	0.1 M $NaNO_3$
34	AMIN	11	8.3	0–123	7.50 ± 0.02	0.1 M $NaNO_3$
63	AMIN	20	8.4	0–567	7.49 ± 0.02	0.1 M $NaNO_3$
69	AMIN	26	8.5	0–57	7.50 ± 0.02	0.1 M $NaNO_3$
71	AMIN	19	25	0–360	6.16 ± 0.02	0.1 M $NaNO_3$
99a	AMIN	16	17	0–230	7.2 ± 0.1	0.01 M $NaNO_3$
99b	AMIN	16	17	0–230	7.2 ± 0.1	0.01 M $NaNO_3$
48	NMIN	19	8.5	0–312	7.05 ± 0.02	0.1 M $NaNO_3$
75	NMIN	32	8.5	0–490	6.20 ± 0.02	0.1 M $NaNO_3$
76	NMIN	31	8.5	0–207	8.15 ± 0.10	0.1 M $NaNO_3$
IS-19	NMIN	8	33	0–35	7.65 ± 0.05	Dauta media
108	Frust. SC	27	Equiv. 36 g/L	0–812	7.10 ± 0.05	0.1 M NaCl
78	Frust. TW	32	Equiv. 35 g/L	0–260	7.48 ± 0.01	0.1 M NaCl
77	Frust. AMIN	19	Equiv. 25 g/L	0–475	6.16 ± 0.02	0.1 M $NaNO_3$
40	SiO_2 am.	14	4 g dry/L	0–766	6.70 ± 0.02	0.01 M NaCl
83	SiO_2 am.	30	4 g dry/L	0–413	6.6 ± 0.1	0.01 M NaCl
pH-dependent adsorption edge						
35–46	SC	28	8.5	51	2.8–9.3	0.1 M $NaNO_3$
59	SC	26	8.5	51	1.7–8.9	0.01 M $NaNO_3$
72	SC	30	8.5	51	2.2–8.8	1 M $NaNO_3$
81	SC	29	8.5	12	1.6–9.2	0.1 M NaCl
118b	SC	20	17	15	2.7–9.4	0.1 M NaCl
119b	SC	16	17	15	3.0–6.2	0.1 M NaCl
42–44	TW	29	8.5	51	3.4–10.5	0.1 M NaCl
51	TW	20	36	61	2.8–10.3	0.1 M NaCl
73	TW	25	70	9	3.4–11.3	0.1 M NaCl
79	TW	38	36	51	2.3–10.3	0.01 M NaCl
80	TW	26	36	51	3.9–8.6	1 M NaCl
30	AMIN	20	8.5	153	2.0–11.2	0.1 M NaCl
31	AMIN	20	35	153	2.3–11.3	0.1 M NaCl
32	AMIN	18	8.5	51	3.3–10.4	0.1 M $NaNO_3$
64	AMIN	24	8.4	51	2.8–10.3	0.001 M $NaNO_3$
65	AMIN	30	8.5	51	2.8–9.6	0.01 M $NaNO_3$
66	AMIN	30	8.5	51	2.8–10.0	1 M $NaNO_3$
67a	AMIN	18	8.5	51	3.2–10.5	0.1 M $NaNO_3$
67b	AMIN	20	8.5	51	3.2–10.7	0.1 M $NaNO_3$
67c	AMIN	18	8.5	51	3.1–9.7	0.1 M $NaNO_3$
68	AMIN	22	8.5	11	2.7–10.1	0.01 M $NaNO_3$
49	NMIN	20	8.5	51	4.0–10.1	0.001 M $NaNO_3$
50	NMIN	30	8.5	51	3.9–9.7	0.1 M $NaNO_3$
61	NMIN	26	8.5	51	2.6–10.1	0.01 M $NaNO_3$
109a/b	NMIN	22	8.5	54	3.0–9.6	0.1 M NaCl
118	NMIN	20	8.5	51	3.1–8.8	1 M $NaNO_3$
52	Frust. TW	18	Equiv. 36 g/L	61	2.8–10.6	0.1 M NaCl
74	Frust. TW	25	Equiv. 70 g/L	9	3.6–10.0	0.1 M NaCl
37	Frust. AMIN	33	Equiv. 35 g/L	153	2.6–9.4	0.1 M NaCl
39	SiO_2 am.	10	4 g dry/L	61	3.0–8.7	0.01 M NaCl

Cell concentration is in g humid/L unless indicated.

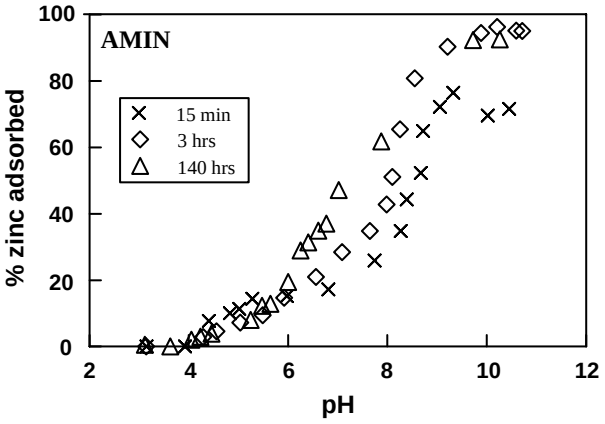

Fig. 4. Effect of exposure time on zinc adsorption on diatoms at 5 °C in the dark. Experimental conditions: biomass equals 8.5 g/L, 0.1 M $NaNO_3$. Cells were exposed during 15 min, 3 h, and 140 h to solution with $[Zn]_o = 51$ μmol/L (Exp. No. AMIN67a, AMIN67b, and AMIN67c, respectively).

tion at $5 \leqslant pH \leqslant 7$ and complete removal of Zn at $pH > 7$–8. At a given pH, the proportion of adsorbed zinc increases with increase of biomass concentration or decrease of $[Zn]_o$ in solution. Below, the effects of major external parameters which are likely to control metal–diatoms interactions such as exposure time, inorganic versus organic cell wall constituents, pH, ionic strength, temperature, and light are described.

The pH-dependent adsorption edges were measured after 5 min, 3 h and 140 h on AMIN species at 5 °C in the dark to prevent the cell growth and biological activity. Results are depicted in Fig. 4. It can be seen that the proportion of adsorbed Zn does not change with time at $pH < 6$, but that the extent of adsorption significantly increases with reaction in weakly alkaline solutions. This is consistent with faster rates of adsorption at low pHs inferred from kinetic measurements (Fig. 1). Increase in the amount of adsorbed zinc with time in weakly alkaline solutions can be explained by: (i) slow incorporation of zinc inside the cells thus renewing surface sites for adsorption and (ii) modification of the diatom cell surface due to long term metal exposure that leads to the production of new surface complexants via detoxification mechanisms (i.e. Ahner et al., 1997; Sunda and Huntsman, 1998). Note, however, that these effects are minor compared to uncertainties attached both to surface groups concentration and surface adsorption constants (see Section 3.3) and thus can be neglected for our first-order description of diatom surface complexation.

To quantify the organic layer contribution during zinc interaction with diatoms, adsorption experiments were conducted first on whole viable cells at a given concentration ($n \times 10^{10}$ cell/L) and then on the same number of frustules ($n \times 10^{10}$ cell/L), which were obtained by quantitative acid digestion of the previous diatom pool. The difference between metal adsorption on the whole cells and corresponding amount of frustules, both for pH-dependent adsorption edge and for Langmurian adsorption isotherm (Fig. 5A–E) demonstrates relatively weak (i.e., $20 \pm 10\%$) contribution of silica skeleton to the overall adsorption of zinc by diatom cells. Note that this value represents the upper limit of frustule contribution to metal binding because organic protein and polysaccharidic layers envelopes the silica membrane from both sides thus decreasing the accessibility of silanol groups to Zn^{2+}(aq).

The effect of ionic strength on pH-dependent adsorption edge for four diatom species is presented in Fig. 6A–D. Overall, the percentage of adsorbed zinc decreases with increasing ionic strength suggesting a competition with sodium for the surface sites or electrostatic effects in the electric double layer. For planktonic species TW, the ionic strength effect is very weak, as the adsorption curves obtained at different electrolyte concentration are very similar. Note that the weak ionic strength dependence for TW is consistent with previous titration experiments (Gélabert et al., 2004) that demonstrated no effect of background electrolyte concentration on TW surface proton adsorption. Zn adsorption on AMIN and NMIN is much more affected by increasing ionic strength.

Compilation of constant pH, Langmurian adsorption isotherms for studied species is presented in Figs. 7A–D. The order of zinc adsorption capacity among different species is SC > NMIN > AMIN > TW. This trend is in agreement with the weight-normalized concentration of surface carboxylate groups for each species: 117, 39, 26 and 24 μmol/g wet weight for SC, NMIN, AMIN, and TW, respectively, as inferred both from proton adsorption and IR measurements (Gélabert et al., 2004). The effect of light exposure on zinc adsorption by viable diatoms is illustrated in Fig. 8. A very slight increase of adsorption under continuous light exposure (6000–8000 lux) witnesses the processes of active uptake occurring in viable cells; however, within the experimental uncertainties, the effect of light can be considered as of second-order importance compared to other environmental parameters.

The effect of temperature on Zn adsorption on freshwater diatoms (AMIN) is illustrated in Fig. 9. The increase of adsorption with temperature observed in the present study is in agreement with available literature data on Cu (Gonzales-Davila et al., 1995, 2000) and Pb (Santana-Casiano et al., 1995) adsorption on marine phytoplankton. This effect can be explained by: (i) positive enthalpy of adsorption reaction (i.e., the enthalpy of $ZnCH_3COO^+$(aq) and $Zn(CH_3COO)_2°$(aq) formation reaction are equal to 8.5 and 22 kJ/mol, respectively, Martell et al., 1997), (ii) specific active biological uptake mechanisms, or (iii) organic surface layers conformation change at low temperatures. However, distinguishing between these mechanisms requires a detailed study of different adsorption-controlling factors at various temperatures.

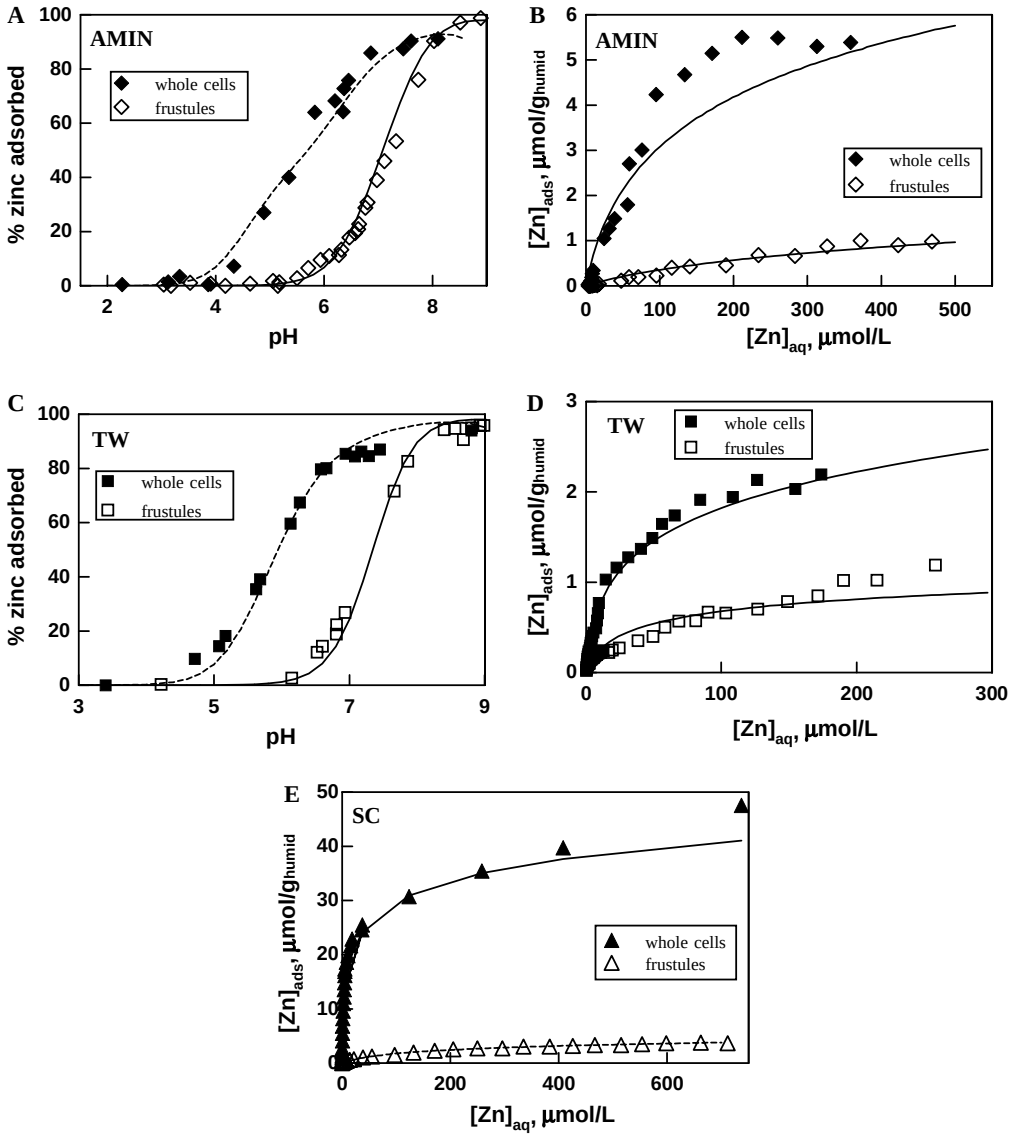

Fig. 5. Adsorption of zinc on whole cells and their frustules as a function of pH and concentration in solution. The frustules were obtained by quantitative digestion of whole cells. Experimental conditions: (A) AMIN, experiments No. 31 and 37, 0.1 M NaCl, $[Zn]_o = 150$ µM, 35 g/L (9.5×10^9 cell/L); (B) AMIN, experiments No. 71 and 77, 0.1 M $NaNO_3$, pH 6.16 ± 0.02, 25 g/L (6.8×10^9 cell/L); (C) TW, experiments No. 73 and 74, 0.1 M NaCl, $[Zn]_o = 9.2$ µM; 70 g/L (3.9×10^9 cell/L); (D) TW, experiments No. 70 and 78, 0.1 M NaCl, pH 7.54 ± 0.06, 35 g/L (1.9×10^9 cell/L); (E) SC, experiments No. 107 and 108, 0.1 M NaCl, pH 7.2 ± 0.1, 36 g/L (1.6×10^{10} cell/L). The symbols represent results of adsorption experiments, but the curves were generated from the surface complexation model (SCM) proposed in this study using thermodynamic parameters listed in Table 2.

3.2. Electrokinetic measurements

Electrophoretic mobilities of AMIN species submitted to an increasing concentration of zinc at pH 7.0 ± 0.1 are depicted in Fig. 10. The diatoms exhibit a constant negative mobility in the full range of investigated $[Zn]_{aq}$ suggesting the dominance of negatively charged functional groups on the surface. Absolute values of electrophoretic mobilities decrease with $[Zn]_{aq}$ at $[Zn]_{aq} > 15$–30 µM, reflecting a decrease of the surface potential due to formation of neutral or positively charged Zn surface complexes (Fig. 10A). Extrapolating these dependencies to $\mu = 0$ allows determination of diatoms isoelectric point in the presence of zinc: pH 7, $[Zn]_{aq} = 1.7 \pm 0.3$ mM. The increase of ionic strength leads to a decrease of the absolute value of the electrophoretic mobilities in the full range of zinc concentration in solution because of the electric double layer compression (Fig. 10A).

No significant difference between the electrophoretic mobilities measured after short (5 min) and long (1–3 h) time exposure to zinc at pH 7 was detected (Fig. 10A). This suggests fast interaction between diatom surface and aqueous zinc ions, already evidenced from adsorption experiments (see Sections 2.2 and 3.1), with no major change of diatom surface speciation occurring upon long-term metal exposure.

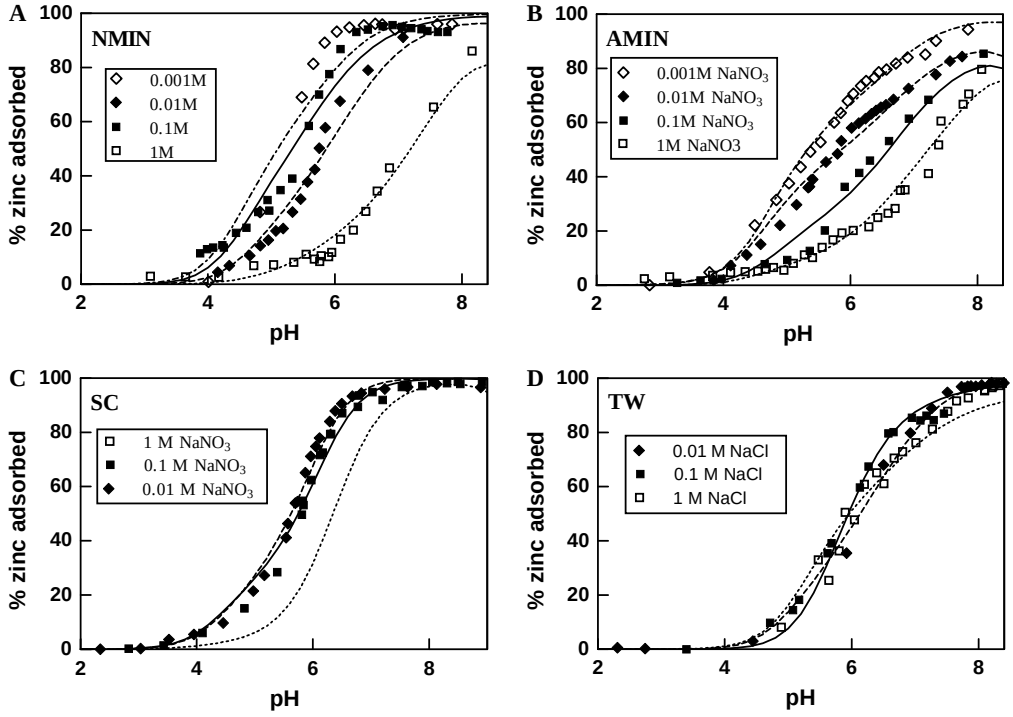

Fig. 6. Percentage of adsorbed Zn as a function of pH at various ionic strengths. Experimental conditions: (A) NMIN, experiments No. 49, 50, 61 and 118, $[Zn]_o = 51$ μM, 8.50 g cells/L; (B) AMIN, experiments No. 32, 64, 65 and 66, $[Zn]_o = 51$ μM, 8.45 ± 0.05 g cells/L; (C) SC, experiments No. 35, 59 and 72, $[Zn]_o = 51$ μM, 8.50 g cells/L; (D) TW, experiments No. 73, 79 and 80, $[Zn]_o = 9$–50 μM, 36.0 g cells/L. The symbols represent results of adsorption experiments, but the curves were generated from the surface complexation model (SCM) proposed in this study using thermodynamic parameters listed in Table 2.

3.3. Surface complexation modeling

In the first part of this study (Gélabert et al., 2004), using a set of spectroscopic and macroscopic techniques, we identified the nature and determine the concentration of the major surface functional groups (carboxylate, amino, and silanol) that control the amphoteric acid–base properties of diatom surfaces. In the circumneutral pH range of adsorption experiments, carboxyl ($pK_a \sim 4$) and silanol ($pK_a \sim 7.5$) are negatively charged while the nitrogen lone pair from amino groups is already involved in proton binding under pH 8, resulting in a positive charge for amine sites. Thus, only carboxyl and silanol groups are likely to bind positively charged Zn^{2+} ions according to the reactions:

$$\gtrdot R{-}COO^- + Zn^{2+} = \gtrdot R{-}COOZn^+, \quad K_{\gtrdot COO{-}Zn} \tag{5}$$

$$\gtrdot SiO^- + Zn^{2+} = \gtrdot SiOZn^+, \quad K_{\gtrdot SiO{-}Zn} \tag{6}$$

In this study, a 1:1 metal–ligand stoichiometry (mononuclear surface complexes) was postulated as follows from EXAFS results on zinc adsorption by diatom surfaces (Pokrovsky et al., 2005a) and in accordance with SCM approaches developed for metal adsorption on bacteria (Fein et al., 1997, 2001; Daughney et al., 1998, 2001). This assumption is based on the fact that the sorption on silanol sites is low compared to carboxylate and the silanols contribution to overall sorption does not exceed 10% (see below). The existence of unique Zn surface site is also supported by the Langmurian plot in log–log units (Fig. 7): at low [Zn] the slope of $[Zn]_{aq}$ vs. $[Zn]_{ads}$ is close to 1.

Following the track developed for metal complexation with bacterial surfaces (Fein et al., 1997; Daughney and Fein, 1998; Fowle and Fein, 1999; Haas et al., 2001), full set of adsorption data was modeled within the framework of the constant capacitance model (CCM) using FITEQL computer code (Herbelin and Westall, 1996). This modeling included optimization of zinc complexation constant with carboxylate and silanol groups and the EDL capacitance value. Note that CCM approach is one among others that is used to model the surfaces of microorganisms in water. For example, it has been recently demonstrated that Non-Electrostatic Model, CCM and Langmuir–Freundlich Model are able to provide equally good fit to the experimental data of proton adsorption on bacterial surfaces (Fein et al., 2005).

Parameters related to "intrinsic" properties of diatom surfaces (pK_a of $\gtrdot R{-}COOH$, $\gtrdot R{-}NH_2$, $\gtrdot SiOH$ and their total concentrations) were allowed to vary only in the range of uncertainties defined in the first part of this study (Gélabert et al., 2004). Reactions (5) and (6) equilibrium constants, $K_{\gtrdot COO{-}Zn}$ and $K_{\gtrdot SiO{-}Zn}$, were optimized at each ionic strength since the surface potential is considered to be independent of electrolyte concentration in the CCM (Sverjensky and Sahai, 1996; Lützenkirchen, 1999). Because the contribution of silanol groups to overall metal

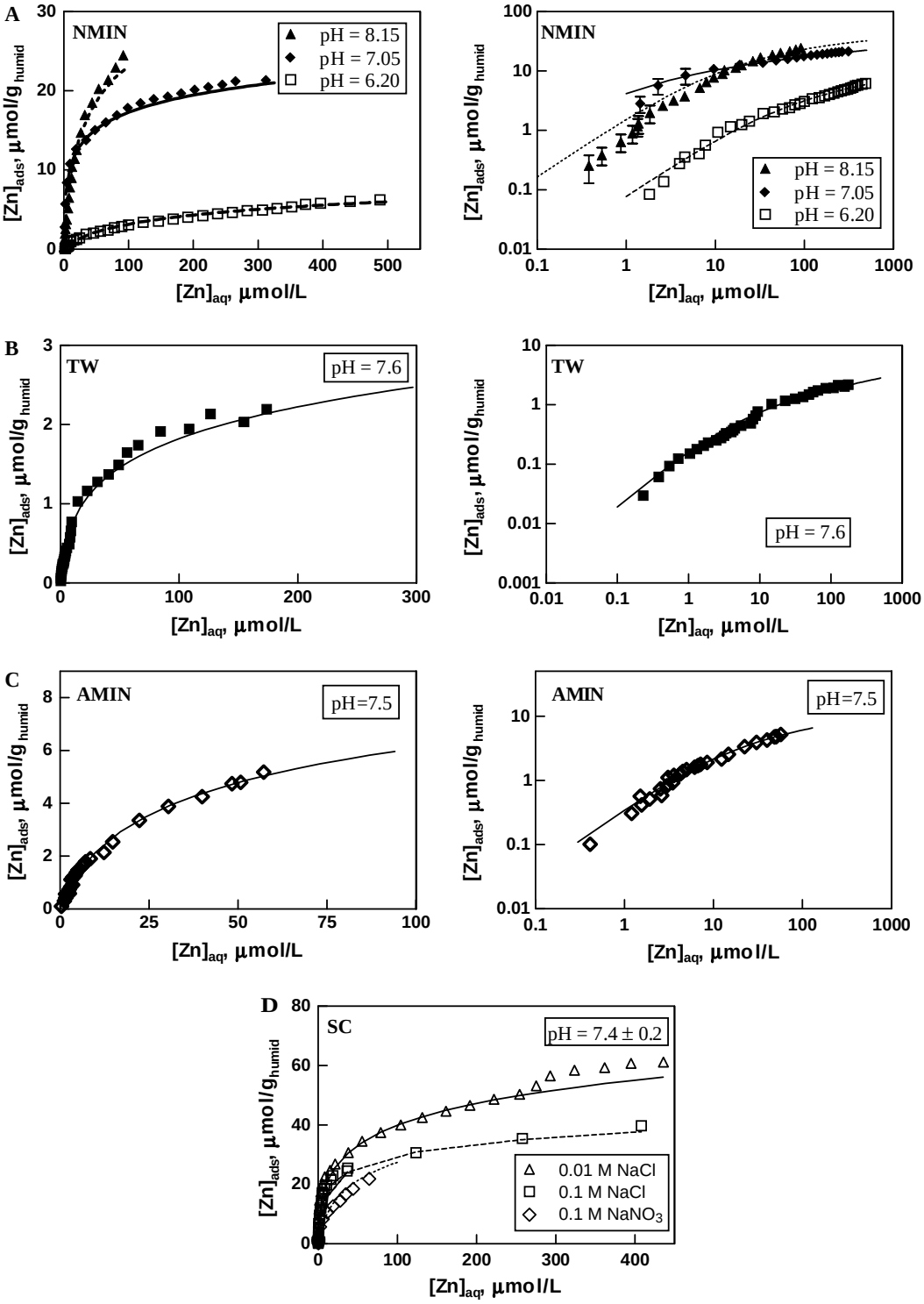

Fig. 7. Concentration of adsorbed zinc as a function of equilibrium zinc concentration in solution (Langmurian adsorption isotherms). Experimental conditions: (A) NMIN, experiments No. 48, 75, and 76, pH 6.20, 7.05, and 8.15, respectively; 0.1 M $NaNO_3$, 8.5 g cells/L; (B) TW, experiments No. 70, pH 7.60; 0.1 M NaCl, 36 g cells/L; (C) AMIN, experiments No. 69, pH 7.50; 0.1 M $NaNO_3$, 8.5 g cells/L; (D) SC, experiments No. 36, 47, and 103, 8.5 g cells/L. The symbols represent results of adsorption experiments, but the curves were generated from the surface complexation model (SCM) proposed in this study using thermodynamic parameters listed in Table 2.

binding to the cell wall is much smaller than that of carboxylic groups (<10 and >90%, respectively), the uncertainties attached to $K_{>SiO-Zn}$ could be much higher compared to those of $K_{>COO-Zn}$. As most investigated diatom species exhibit clear dependence of Zn adsorption on ionic strength (Fig. 6), significant improvement of fit was obtained by introducing zinc competition with sodium for surface carboxylate groups:

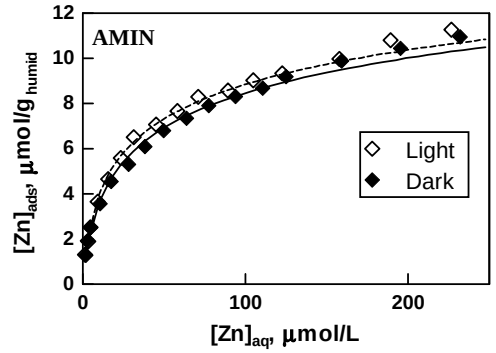

Fig. 8. Langmurian adsorption isotherms of zinc on AMIN cells under light (open diamonds, Exp. No. AMIN99a) and in the darkness (solid diamonds, Exp. No. AMIN 99b). Experimental conditions: 17 g cells/L, 0.01 M $NaNO_3$, pH 7.2 ± 0.1, exposure time equals 3.5 h.

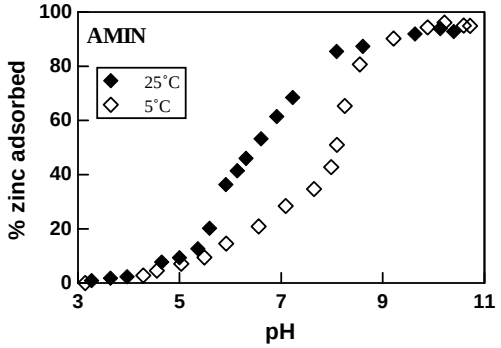

Fig. 9. Zinc adsorption on AMIN cells as a function of pH at 5 °C (open diamonds, experiment No. 32) and 25 °C (solid diamonds, experiment No. 67b) in 0.1 M $NaNO_3$. Cell concentration = 8.5 g humid/L, $[Zn]_o$ = 51 µM, exposure time = 3 h in the dark.

$$\geq R{-}COO^- + Na^+ = \geq R{-}COONa^\circ, \quad K_{\geq COO{-}Na} \qquad (7)$$

Mechanistically, reaction (7) accounts for the competition between Zn^{2+} and Na^+ for the same surface sites as the proportion of adsorbed Zn decreases with increase $[NaNO_3]$ or [NaCl] (Figs. 6A–C). In the case of electrostatic effects, the adsorption edge would have shifted in opposite direction with increase of I due to surface negative charge increase and stronger attraction. Therefore, the stability constant of reaction (7) was treated as additional adjustable parameters for both freshwater and marine species. Note that acid–base surface titrations performed in the first part of this study (Gélabert et al., 2004) did not allow quantification of reaction (7) due to insufficient amount of measurements at various ionic strengths. The sensitivity of the model to $K_{\geq COO{-}Na}$ is low: a change of ±0.2 $\log K_{\geq COO{-}Na}$ leads to a ±10% uncertainty in the amount of sorbed Zn (in Langmurian isotherm) or a ±5% uncertainty in the proportion of adsorbed Zn (in pH-dependent adsorption edge). Therefore, only rough estimation of this constant was possible and special experiments on Na^+ adsorption are necessary to precisely determine $K_{\geq COO{-}Na}$ value.

Full set of SCM parameter values and average recommended values in this study for Zn–diatom surface interaction are listed in Tables 2 and 3, respectively. Surface stability constants listed in these tables represent conditional values for a given ionic strength (Table 2) and recommended values in the range of ionic strength 0.001–1.0 M (Table 3), respectively. In agreement with previous studies of zinc complexation with bacteria (Fein et al., 2001), algae (Xue et al., 1988; Gonzalez-Davila, 1995) and silica (Dellolme et al., 2004), and sodium complexation with carboxylate groups of humic acids (Westall et al., 1995), the pK of intrinsic surface stability constants for reactions (5)–(7) were initially fixed as 4.5, 3.0, and 1.5, respectively. Results of each adsorption experiment were fitted individually by varying surface reaction constants by not more than 1.0 log units from the initial values to provide simultaneously a best fit of the experimental pH-dependent adsorption edge and the "Langmurian" adsorption isotherm.

The goodness of model fit to a data set is represented by the overall variance ($V(Y)$) calculated by FITEQL. This variance is normalized with respect to the number of experimental data points, the number of chemical components for which the total concentration is known and the number of adjustable parameters. Generally, a value of $V(Y)$ less than 20 corresponds to a good fit (Herbelin and Westall, 1996), although it has been argued that graphical goodness of fit should be preferred over numerical goodness of fit parameters (Gunneriusson and Sjoberg, 1993). The overall

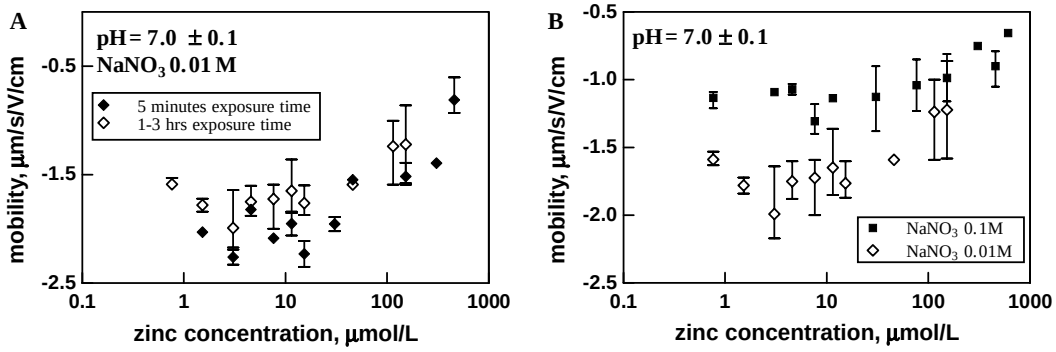

Fig. 10. Electrophoretic mobility of AMIN cells at pH 7.0 as a function of zinc concentration in solution for different exposure time in 0.01 M $NaNO_3$ (A) and different ionic strengths after 3 h exposure (B).

Table 2
Summary of SCM parameters for Zn–diatom surface interaction

Exp. No.	Species	Electrolyte	≥COOH pK_{a1}	≥NH_2 pK_{a3}	≥SiOH pK_{a2}	log K_{COOZn}	log K_{SiOZn}	log K_{COONa}	[≥COOH] (mol/g_{humid})	[≥NH_3] (mol/g_{humid})	[≥SiOH] (mol/g_{humid})	C, F/g	$V(Y)$
Langmurian adsorption isotherm													
36	SC	0.1 M $NaNO_3$	−4.80	8.10	ND	5.16	ND	0.30	1.04E−04	1.96E−04	ND	62	39
47	SC	0.1 M NaCl	−4.80	8.20	ND	5.30	ND	0.20	1.13E−04	1.53E−04	ND	62	29
103	SC	0.01 M NaCl	−4.80	8.10	ND	5.54	ND	0.30	1.79E−04	1.96E−06	ND	75	89
107	SC	0.1 M NaCl	−4.80	8.20	ND	5.32	ND	0.20	1.78E−04	1.96E−04	ND	100	161
70	TW	0.1 M NaCl	−4.90	9.70	−7.00	4.61	2.80	0.41	2.40E−05	2.55E−05	1.94E−06	6	2.2
33	AMIN	0.1 M $NaNO_3$	−4.80	9.70	−7.10	4.32	3.20	0.50	2.94E−05	2.40E−05	1.40E−05	37	80
34	AMIN	0.1 M $NaNO_3$	−4.80	9.80	−7.10	4.23	3.20	0.32	2.95E−05	2.41E−05	7.47E−06	31	5.0
63	AMIN	0.1 M $NaNO_3$	−4.80	9.8	−7.10	4.22	3.20	0.80	2.94E−05	2.40E−05	1.65E−05	38	21
69	AMIN	0.1 M $NaNO_3$	−4.80	9.80	−7.10	4.24	3.20	0.56	2.82E−05	2.81E−05	1.03E−05	25	0.9
71	AMIN	0.1 M $NaNO_3$	−4.80	9.80	−7.10	4.24	3.20	0.65	2.60E−05	2.81E−05	1.03E−05	25	70
99a	AMIN	0.01 M $NaNO_3$	−4.80	10.20	−7.00	4.28	3.20	1.00	2.24E−05	2.41E−05	1.86E−05	35	3.4
99b	AMIN	0.01 M $NaNO_3$	−4.80	10.20	−7.00	4.26	3.20	1.00	2.24E−05	2.41E−05	1.86E−05	35	3.4
48	NMIN	0.1 M $NaNO_3$	−4.80	8.30	−6.60	5.26	3.00	0.39	4.11E−05	4.20E−05	1.60E−05	30	14
75	NMIN	0.1 M $NaNO_3$	−4.80	8.40	−6.60	5.05	3.00	1.25	3.71E−05	4.40E−05	1.00E−05	12	1.0
76	NMIN	0.1 M $NaNO_3$	−4.80	8.50	−6.60	5.00	3.00	1.25	4.11E−05	4.20E−05	1.60E−05	87	39
108	SC frustules	0.1 M NaCl	ND	ND	−7.00	ND	3.2	ND	ND	ND	1.06E−03	840	9.6
78	TW frustules	0.1 M NaCl	ND	ND	−7.00	ND	2.80	ND	ND	ND	1.33E−03	404	7.2
77	AMIN frustules	0.1 M $NaNO_3$	ND	ND	−7.10	ND	3.2	ND	ND	ND	4.32E−04	70	2.5
35–46	SC	0.1 M $NaNO_3$	−4.80	8.20	ND	5.32	ND	0.20	1.59E−04	1.96E−04	ND	47	1.7
59	SC	0.01 M $NaNO_3$	−4.80	8.00	ND	5.20	ND	0.20	1.58E−04	1.96E−04	ND	50	1.5
72	SC	1 M $NaNO_3$	−4.80	8.20	ND	5.33	ND	0.20	1.53E−04	1.96E−04	ND	37	1.1
81	SC	0.1 M NaCl	−4.80	8.20	ND	5.32	ND	0.20	1.35E−04	1.97E−04	ND	40	0.7
51	TW	0.1 M NaCl	−4.90	9.70	−7.00	4.69	2.80	0	2.32E−05	2.56E−05	1.28E−06	3	24
73	TW	0.1 M NaCl	−4.90	9.70	−7.00	4.70	2.80	0	2.40E−05	1.99E−06	1.28E−06	2	0.1
79	TW	0.01 M NaCl	−4.90	9.70	−7.40	4.75	2.80	0	2.40E−05	2.50E−05	4.06E−06	3	0.7
80	TW	1 M NaCl	−5.05	9.80	−7.20	4.72	2.80	<0 (ND)	2.40E−05	2.50E−05	4.06E−06	12	5.0
30	AMIN	0.1 M NaCl	−4.80	9.70	−7.10	4.36	3.20	0.60	2.94E−05	3.21E−05	1.87E−05	25	24
31	AMIN	0.1 M NaCl	−4.80	9.70	−7.10	4.40	3.20	0.60	2.94E−05	3.09E−05	1.87E−05	17	19
32	AMIN	0.1 M $NaNO_3$	−4.80	9.70	−7.10	4.24	3.20	0.32	2.94E−05	3.07E−05	1.87E−05	17	4.4
64	AMIN	0.001 M $NaNO_3$	−4.80	9.80	−7.00	4.23	3.20	0.87	2.94E−05	2.42E−05	1.87E−05	25	0.8
65	AMIN	0.01 M $NaNO_3$	−4.80	10.20	−7.00	4.26	3.20	1.00	2.95E−05	2.98E−05	1.87E−05	35	2.0
66	AMIN	1 M $NaNO_3$	−4.80	8.30	−7.00	4.45	3.20	0.60	2.94E−05	2.40E−05	1.87E−05	22	8.8
68	AMIN	0.01 M $NaNO_3$	−4.80	10.20	−7.00	4.29	3.20	1.00	2.74E−05	2.55E−05	1.87E−05	30	3.8
49	NMIN	0.001 M $NaNO_3$	−4.80	8.70	−6.66	5.01	3.00	1.09	4.11E−05	4.20E−05	1.60E−05	17	8.1
50	NMIN	0.1 M $NaNO_3$	−4.80	8.40	−6.60	5.07	3.00	0.32	4.11E−05	4.20E−05	1.60E−05	12	6.9
61	NMIN	0.01 M $NaNO_3$	−4.80	10.00	−6.90	5.00	3.00	0.37	3.87E−05	4.20E−05	1.60E−05	10	3.3
109a/b	NMIN	0.1 M NaCl	−4.80	8.40	−6.60	5.00	3.00	0.94	3.71E−05	4.40E−05	1.00E−05	12	1.8
118	NMIN	1 M $NaNO_3$	−4.80	8.40	−6.60	5.07	3.00	0.32	3.71E−05	4.36E−05	1.00E−05	7	4.8
74	TW frustules	0.1 M NaCl	ND	ND	−7	ND	2.79	ND	ND	ND	1.19E−03	404	0.2
37	AMIN frustules	0.1 M NaCl	ND	ND	−7.1	ND	3.21	ND	ND	ND	4.32E−04	70	5.2

pK_{a1}, pK_{a2}, and pK_{a3} are taken from Gélabert et al. (2004) and the other parameters are determined in the present work. ND means non determined.

Table 3
Average recommended parameters of constant capacitance, surface complexation model used to describe Zn–diatoms interactions in aqueous solutions at 25 °C

Species	$\log K_5$ ($\equiv$R–COOZn$^+$)	$\log K_6$ ($\equiv$SiO–Zn$^+$)	$\log K_7$ ($\equiv$R–COONa^o)	[$\equiv$COOH] (μmol/g humid)	EDL capacitance (F/g)
Skeletonema costatum	5.31 ± 0.11	ND	0.23 ± 0.05	147 ± 28	59 ± 21
Thalassiosira weissflogii	4.69 ± 0.06	2.8 ± 0.1	0.0 ± 0.1	23.6 ± 0.5	3.4 ± 1.9
Achnanthidium minutissimum	4.29 ± 0.07	3.2 ± 0.1	0.70 ± 0.24	28 ± 3	28 ± 7
Navicula minima	5.07 ± 0.09	3.0 ± 0.1	0.67 ± 0.41	39 ± 2	15 ± 2

Table 4
Results of stable isotopic fractionation

Sample description	Duration of exposure	pH	$[Zn]_{aq}$ (μmol/L)	[DOC] (mg/L)	% Zn adsorbed	$\delta^{66}Zn_{aq}$ (‰)	$\delta^{66}Zn_{solid}$ (‰)	$\Delta^{66/64}Zn_{solid-solution}$ (‰)
(1) Long-term uptake in growing cells (20 °C, under light)								
AMIN	3 weeks	7.75 ± 0.25	0.3 ± 0.004	8.0	ND	0.12	0.31	0.19
NMIN	3 weeks	7.75 ± 0.25	0.3 ± 0.004	8.0	ND	0.12	0.33	0.21
TW	3 weeks	7.75 ± 0.25	0.3 ± 0.004	10.0	ND	0.12	0.39	0.27
SC	4 weeks	7.95 ± 0.25	0.3 ± 0.004	15.0	ND	0.12	0.20	0.08
(2) Short-term adsorption on growing cells from culture media (20 °C, under light)								
NMIN N 7	3.5 h	8.14	2.5	3.9	67	-0.19 ± 0.1	0.27	0.47
NMIN N 5	16 h	8.03	4.7	2.9	74	-0.10 ± 0.1	0.23	0.33
NMIN N 6	42 h	7.64	6.0	3.1	67	-0.25 ± 0.1	0.25	0.50
AMIN N 3	20 min	7.85	1.4	3.5	70	-0.08 ± 0.1	0.21	0.29
AMIN N 2	19 h	7.80	5.0	3.1	73	-0.06 ± 0.1	0.19	0.24
(3) Reversible adsorption on frustules ($SiO_2 \cdot nH_2O$) of NMIN in 0.01 M $NaNO_3$ (25 °C, in the dark)								
NF–18	20 h	5.37	20	<0.2	15	0.084	0.33	0.25
NF–19	20 h	5.43	17	<0.2	26	0.052	0.31	0.26
NF–20	20 h	5.57	14	<0.2	39	−0.038	0.36	0.40
NF–9	20 h	5.62	5.4	<0.2	73	−0.206	0.24	0.48

In the initial Zn salt $\delta^{66}Zn_{initial} = 0.12 \pm 0.05$‰. Uncertainty on $\delta^{66}Zn$ is 0.05‰ unless indicated.

variances calculated for each experiment are listed in Table 2; it can be seen that for most experiments $V(Y) \leqslant 20$ which indicates a good adherence to experimental data of predicted adsorbed concentration.

The EDL capacitance value, C, which could not be fitted by FITEQL, was initially fixed for each species according to our previous determination of diatom surface acidity constants (Gélabert et al., 2004). However, it was revealed that optimization of C allows significant improvement of the fit. New optimized EDL capacitances listed in Table 2 are about four and ten times lower than those extracted from acid–base titrations for AMIN, NMIN, TW, and SC, respectively. Although C value for porous 3D multilayer diatom cell surface should be considered as a purely adjustable parameter without rigorous physical meaning, one can hypothesize that the decrease in EDL capacitance arises from weaker electrostatic effects associated with Zn sorption than with proton/hydroxyl penetration occurring during acid–base titrations of diatoms. Note that lower C values for Zn adsorption are also consistent with lower surface adsorption densities for Zn (0.4–4 mg/g humid or 6–50 μmol/g humid, Fig. 7) compared to those for protons (20–120 μmol/g humid, Gélabert et al., 2004). However, the slightly different models used for protons (pure CCM) and Zn adsorption (CCM with competition between Zn and Na for $\equiv$R–COO$^-$) might partly account for the different C values. The sensitivity of the model fit to C value within the range postulated in this study is comparable with the experimental reproducibility: for example, the difference in C value between 10 and 1 F/g yields only ±10% difference in Zn adsorption at pH ~ 6, which is not very far from the actual experimental reproducibility. Note that the absolute value of C between different species or between the cells and the frustules cannot be compared. This is related to normalization of site densities in capacitances per mass of diatoms. For example, *S. costatum* exhibits the highest site densities, capacitances, cell wall thickness and frustule specific surface area.

Results of Zn adsorption modeling are illustrated in Figs. 5–8 where dashed or solid lines give predicted sorption of zinc as a function of pH or Zn aqueous concentration. It can be seen from these figures that, despite the large dataset used to generate the model parameters and the relative simplicity of our model, the agreement between calculated and measured values is rather good. Some difficulties to accurately describe the experimental data have been encountered for experiments No. 71, 107, and 49 (underestimation of Zn sorption at high [Zn]), 75 and 76 (overestimation of sorbed Zn at low [Zn]). Very often, this disagreement is within ±10–20% which is comparable with real experimental reproducibility.

It has been suggested in previous works on algae that there is a small amount of high-affinity sites that are able to effectively complex/adsorb the metal at low metal/biomass ratio (Gonzalez-Davila; Goncalves et al., 1987; Xue et al., 1988). To test this hypothesis for diatoms, the fitting of adsorption curves at low $[Zn^{2+}]_{aq}$ was tested with additional "low-abundant" sites of high affinity for Zn. The concentration of such sites was assumed to be 10–1000 times less than that of carboxylate groups whereas the logarithm of Zn sorption constant on these sites was allowed to vary between 6 and 8. Addition of these high-affinity sites did not improve the quality of experimental data description and, in many cases, the fit convergence was not achieved.

Taking into account of the formation of Zn–DOC complexes in aqueous solution also did not allow fit improvement. Indeed, for most of experiments, the concentration of DOC (~2–4 μM) is more than two orders of magnitude lower than that of the cell binding sites (~200–1000 μM). Because the stability constants of Zn complexation with carboxylic groups of DOC exudates and cell surfaces are similar, it is unlikely that significant proportion of Zn is complexed with organic carbon in solution.

3.4. Stable isotope fractionation

Results of stable isotope measurements are reported in Table 4. Analyses of digested cells from two independent series of diatom culturing experiments in the presence of Zn agree within the uncertainty of analysis and demonstrate a clear enrichment of cells in heavy isotope. The isotopic offset Δ^{66}Zn(solid–solution) is equal to 0.19 ± 0.05, 0.21 ± 0.05, 0.27 ± 0.05, and 0.08 ± 0.05‰ for AMIN, NMIN, TW, and SC, respectively. For adsorption experiments on living cells at pH 7.6–8.1, systematic enrichment of cells in heavy isotope, which is independent of exposition time (20 min to 42 h), is observed; Δ^{66}Zn(solid–solution) is equal to 0.27 ± 0.10 and 0.43 ± 0.10‰ for AMIN and NMIN, respectively. Following its adsorption on frustules of *N. minima* at $5.4 \leqslant pH \leqslant 5.6$ Zn is also enriched in ^{66}Zn (Δ^{66}Zn(solid–solution) $= 0.35 \pm 0.05$‰). Extent of this "biological" isotopic fractionation is higher than that induced by Zn sorption on inorganic materials such as goethite, birnessite, pyrolusite, corundum, and $Al(OH)_3$: Δ^{66}Zn(solid–solution) $= -0.20 \pm 0.03$, -0.17 ± 0.06, 0.10 ± 0.03, 0.10 ± 0.09, 0.13 ± 0.12‰, respectively (Pokrovsky et al., 2005b). Overall, zinc stable isotopic fractionation induced by adsorption on most mineral surfaces does not exceed 0.2‰. However, the isotopic shift induced by Zn sorption on ferrihydrite and hematite, can achieve +0.6‰ (Cacaly et al., 2004; Pokrovsky et al., 2005b).

4. Discussion

For all studied species, a two sites (carboxyl and silanol) model that is based on previously measured site densities and protonation constants, provides an accurate description of the sorption data (i.e., see Figs. 5–8). For *S. costatum*, very low contribution of silica to cell wall functional groups was demonstrated from metal-free system studies (Gélabert et al., 2004), and the adsorption data fitting did not require introducing reaction (6) in the model. For this species, the fitting of all adsorption data required amino groups concentration by an order of magnitude lower than that obtained from acid–base titration. This can be explained by the fact that the cell wall of SC has the highest thickness of porous organic layer (Gélabert et al., 2004). Because zinc adsorption onto SC is likely to occur on the most external polysaccharidic layers of the cell wall, a large amount of amino groups, located beneath the silica frustule (Hecky et al., 1973), do not contribute to surface charge and metal complexation in the circumneutral pH range. In accordance with quantitative macroscopic measurements of the present study (Fig. 5), mainly carboxyl groups are involved in zinc binding on the cell surface while silanol sites contribution from the frustule are much less important.

The model elaborated in this study on the basis of surface adsorption data also allows satisfactory representation of surface electric potential as inferred from electrophoretic mobility measurements (Fig. 10). In the full range of investigated $[Zn]_{aq}$ and at pH ~ 7, the cell outermost layers remain negatively charged due to the dominance of $\equiv COO^-$ groups. According to model prediction, at $[Zn]_{aq} > 15$–30 μM, $[\equiv COOZn^+]$ species starts to contribute to the surface potential, accounting for 10–20% of the surface sites, in agreement with measurements of electrophoretic mobilities (Fig. 11).

It has been argued that a number of microorganisms exhibit similar proton and metal binding constants leading to so-called "universal" adsorption edge. For example, a single pH-dependent Cd adsorption edge has been observed in laboratory experiments using individual strains of bacteria (Yee and Fein, 2001) and natural bacteria consortia (Borrok et al., 2004). In this study, we compared Zn adsorption on the four diatom species by plotting: (i) the percentage of adsorbed zinc as a function of pH

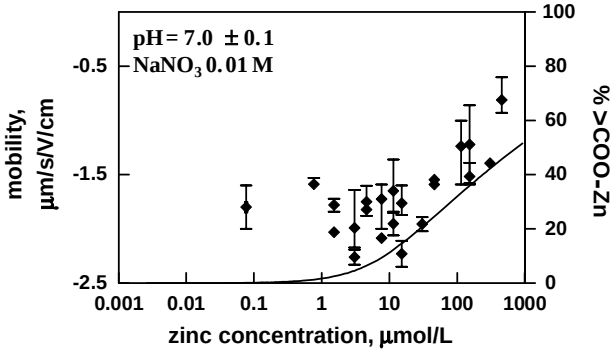

Fig. 11. Electrophoretic mobilities of AMIN species as a function of zinc concentration in solution measured in 0.01 M $NaNO_3$ at pH 7.0 (symbols) and SCM prediction of the molar percentage of $\equiv R–COOZn^+$ species on the outermost surface layer (solid line).

(Fig. 12A) and (ii) the concentration of adsorbed zinc as a function of $[Zn]_{aq}$ at constant pH (Fig. 12B). While semi-logarithmic pH-dependent adsorption edge (Fig. 12A) is, indeed, rather similar among the four species studied, a "Langmurian" adsorption isotherm plot (Fig. 12B) reveals significant differences between species related to specific properties of metal binding reactions and weight-normalized site concentrations. Simultaneous pH-edge and Langmurian isotherm experiments are necessary to assess the metal binding capacities of microorganisms.

While the maximal Zn adsorption densities are different among all four species, the values of the main surface adsorption constant ($K_{\equiv COO-Zn}$, reaction (5)), are of the same order of magnitude: the average value for all experiments yields $\log K_{\equiv COO-Zn} = 4.8 \pm 0.3$. Zinc-carboxylate group interaction with a similar value of formation constant is widely used for modeling of this metal binding by algae (Schiewer and Volesky, 1995; Kiefer et al., 1997) and bacteria surfaces (Ngwenya et al., 2003; Borrok et al., 2004). In some studies with bacteria, reported values for this stability constant are an order of magnitude lower (i.e. Plette et al., 1996; Fein et al., 2001; Ngwenya et al., 2003) than the value determined for diatoms in the present work. The reason for this is the different nature of surface groups involved in Zn and other metals binding by different microorganisms. Indeed, the set of SCM parameters used by the last authors for bacteria implies complexation with strongly-binding phosphate groups ($\log K_{Zn-PO4} \sim 5$) while the adsorption on carboxylate sites ($\log K_{Zn-COO} \sim 3.5$) occurs mostly at high pHs. Spectroscopic observations also evidenced important role of phosphate moieties in Zn binding by bacterial cells (Webb et al., 2001; Boyanov et al., 2003). In bacterial cells, rigidity is brought by peptidoglycan of cell wall that contains secondary polymers (e.g., teichoic acid) having phosphoryl functions and exhibiting high affinity for metals (Beveridge, 1988; Beveridge et al., 1997). In diatoms, the role of peptidoglycan is partially played by silica frustule that also contributes to metal binding by the cell wall (reaction (6)). Our spectroscopic and macroscopic measurements did not evidence the presence of phosphate groups in diatoms cell envelopes (i.e., their proportion is less than 1% of surface carboxylates, Gélabert et al., 2004). Moreover, the addition of these phosphate groups for modeling Zn surface binding did not allow the fit to converge. Finally, our recent X-ray absorption spectroscopy (XAS) study of zinc adsorption on diatom surfaces did not evidenced the presence of phosphorus in the second neighbor environment and confirmed monodentate mononuclear or binuclear binding to carboxylate groups of the surface layer (Pokrovsky et al., 2005a). Recently, Zn monodentate complexes with carboxyl have been identified in Gram-negative bacteria (Guiné et al., 2005).

The overall Zn binding capacities of diatom surfaces measured in the present study (100–500 μmol/g dry weight) are in good agreement with recent measurements of Klimmek et al. (2001) on 30 algae (100–400 μmol/g dry weight) and diatoms (230 μmol/g dry weight). The order of Zn binding capacity of diatoms cell wall (SC > NMIN > AMIN > TW) assessed in the present work is consistent with our previous attenuated total reflection (FT-ATR) results of carboxylate group concentration in the surface layers (Gélabert et al., 2004).

The value of the constant for sodium–zinc exchange on diatoms surface ($\equiv COO-Zn^+ + Na^+ = \equiv COO-Na^\circ + Zn^{2+}$) proposed in this study, $\log K_{exch} = \log K_{\equiv COO-Na} - \log K_{\equiv COO-Zn}$, varies between −2 and −3, in agreement with the value −2.1 found for other algae (*Vaucheria*, Crist et al., 1981). Because Zn adsorption on freshwater species is much more affected by increasing Na concentration than that on marine species (Section 3.1), the stability constant for sodium adsorption on carboxylate groups ($\log K_{\equiv COO-Na}$) is lower for SC and TW (~0.1–0.2) compared to AMIN and NMIN (~0.7–1.2). It follows both from spectroscopic observations and quantitative macroscopic measurements that marine planktonic diatoms contain much less amount of silica in their cell wall (Gélabert et al., 2004). It is known that, for silica, the counter Na^+ ions can closely approach the potential determining OH/O^- groups (Iller, 1979). As a result, sodium can compete with Zn for surface sites (both silanol and carboxylate) of freshwater diatoms, but exhibit much less effect on marine species. Thus the structural

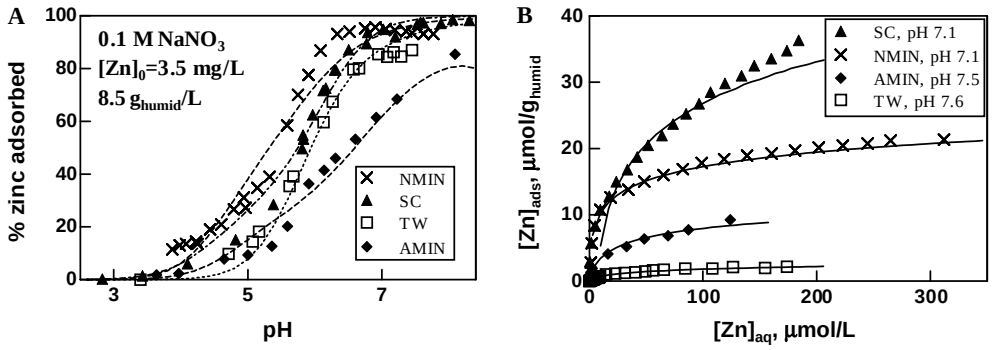

Fig. 12. Comparison of zinc adsorption among the four diatom species: (A) pH-dependent adsorption edge (experiments No. 32 (AMIN), 50 (NMIN), 73 (TW) and 35 (SC)) at $[Zn]_o = 54$ μM, $I = 0.1$ M and cell concentration equals 8.5 g/L. (B) "Langmurian" adsorption isotherm (experiments No. 34 (AMIN), 48 (NMIN), 70 (TW) and 47 (SC)) at $I = 0.1$ M and pH 7.3 ± 0.2.

differences in the cell walls are the primary factors controlling the different ionic strength effect for the different species. The effect of NaCl on Zn adsorption on TW cells is the lowest among all studied species (Fig. 6D). *T. weissflogii* is the only estuarine species that lives under conditions of variable salinity. It is possible that specific biochemical/organo-chemical characteristics such as protein and polysaccharides conformation on TW surface are responsible for the weak effect of salinity on Zn affinity to cell surface which is necessary for maintaining need for Zn homeostasis requirement under variable external media.

Note that the possible reaction between Na and silanol groups has not been considered in this study. This reaction would complicate the model without providing any predictive ability to the SCM. The tests we performed for species NMIN which have the highest proportion of SiO_2 in their cell wall (Exp. Nos. 61, 75, and 109) demonstrated that either the fit did not converge at all or its goodness was not improved. Because the sensitivity of the model description to reaction (7) is already very low (see also Section 3.3), the addition of reaction between $\equiv SiO^-$ and Na^+ would not allow the resolving of its stability constant.

Measurements of zinc stable isotopes fractionation performed, for the first time, on diatoms and their silica frustules interacting with aqueous solutions, revealed systematic enrichment of cells in heavy isotope (Table 4). The ^{66}Zn enrichment can be explained by the change of Zn coordination upon its reaction with diatoms: Zn is coordinated to six water molecules in aqueous solution but it reduces its coordination to four in the complexes it forms with carboxylate, amine or silanol groups inside or on the surface of the cells (Pokrovsky et al., 2005a). Enrichment of ^{66}Zn in diatoms is consistent with results of quantum mechanical calculations which predict that the heavier isotope should concentrate in the species in which it is bounded most strongly (Criss, 1999), i.e., tetrahedral Zn–carboxylate or silanol complexes with shorter Zn–O bonds. However, one cannot establish a simple correlation between the EXAFS-based shift in Zn first neighbor bond distances between diatoms, their frustules and aqueous solution (Pokrovsky et al., 2005a) and $\Delta^{66}Zn$(solid–solution) measured in this study. As recently shown for B isotopes fractionation upon sorption on humic acid and metal oxides (Lemarchand et al., 2005), results of surface complexation modeling may serve as a useful guide for assessing the degree of isotopic fractionation. Indeed, the difference in isotopic offset $\Delta^{66}Zn$(solid–solution) between AMIN and NMIN species (0.27 and 0.43‰, respectively) exhibits the same trend as the difference in Zn surface adsorption constants on these diatoms ($\log K_{\equiv COO-Zn} = 4.25$ and 5.0, respectively). The isotopic offset for NMIN frustules is lower than that for viable cells *N. minima*, and the surface adsorption constant is, accordingly, lower ($\log K_{\equiv SiO-Zn} < \log K_{\equiv COO-Zn}$, Table 2). Thus it can be advocated that, in the case of diatoms, for equivalent surface complexes, the higher the adsorption constant, the larger the isotopic fractionation if the metal is more strongly bonded in the surface species than in the aqueous species.

5. Conclusions

This study allows comprehensive and quantitative description of zinc adsorption on diatom surfaces. Various "external" parameters such as pH, zinc and biomass concentration in solution, ionic strength and temperature are likely to govern Zn binding by diatom cells. Like most processes of "passive" metal adsorption on organic and inorganic materials, zinc interaction with viable diatoms is very fast and largely reversible, thus it allows to use a thermodynamic approach for modeling zinc surface complexation reactions. Overall, the metal binding properties of diatom surfaces measured in the present study are comparable with those for bacteria, algae and other biological materials. The role of silica frustule, estimated from comparison of sorption experiments on whole cells and their silica exoskeletons, is relatively small and cannot exceed 30% of overall metal binding. As a result, the majority of diatom-trapped metals, located in the organic coating, are likely to be released in the environment during diagenesis of diatom cells.

Results of FITEQL thermodynamic modeling of adsorption demonstrated that the major surface functional groups responsible for Zn binding by diatoms are carboxylate moieties located in the external polysaccharidic layers of the cell wall or the proteins side chains. No complexation with phosphoryl groups of surface layer was required to model Zn adsorption on diatoms, in agreement with previous XAS study. For freshwater species, competition between Zn^{2+} and Na^+ for $\equiv COO^-$ sites leads to significant decrease of metal adsorption in solutions of high ionic strength. In agreement with previous results on bacteria, pH-dependent adsorption edge is almost the same for the four diatom species. The reaction constants for Zn adsorption on carboxylate sites are of the same order of magnitude (the average value for all experiments yields $\log K_{\equiv COO-Zn+} = 4.8 \pm 0.4$). However, Langmurian adsorption plots, and, accordingly, Zn surface adsorption capacities are very different among species. This should be taken into account for quantitative biogeochemical modeling of metal "passive" adsorption by diatom cells.

The present study represents only a first-order macroscopic characterization of metal interactions with diatom surfaces. Nevertheless, together with previous studies of metal speciation on the surface and in solution (e.g. Gonzales-Davila et al., 1995; Santana-Casiano et al., 1997), and analysis of metal uptake and transport by marine diatoms (Phinney and Bruland, 1994; Sunda and Huntsman, 1998), it provides a basis for the quantitative physico-chemical description of zinc interaction with planktonic and periphytic diatoms. More comprehensive analysis of active metal uptake processes and internalization fluxes via irreversible penetration inside the cells like that elaborated

for green algae and bacteria (Mirimanoff and Wilkinson, 2000; Slaveykova and Wilkinson, 2002; Smiejan et al., 2003; Kola and Wilkinson, 2005) is not available for diatom species and will be a goal for further research.

The change of zinc isotopic composition during its incorporation and adsorption on viable diatoms and their frustules assessed, for the first time, in this work, provides important constraints on biological fractionation mechanisms in surficial aquatic environments. A systematic isotopic offset of $\Delta^{66}Zn(\text{solid–solution}) = 0.3 \pm 0.1‰$ is expected when Zn is scavenged by diatoms from aqueous solution. New measurements of Zn isotopic composition in rivers, seawater, plankton and periphyton are necessary to compare these laboratory results with Zn geochemistry in natural settings and to test the tracks open in this study by Zn isotopes in the tracing of biogeochemical processes.

Acknowledgments

We are grateful to J. Fein and three anonymous reviewers whose insight and thorough reviews greatly improve the manuscript. This work was supported by the French National Programs for Basic Research ACI "Eau et Environnement" and ECODYN (Ecodynamique et Ecotoxicologie des Contaminants). We thank B. Etcheverria for invaluable help during diatom culture process. Participation of C. Gold at several stages of this work is equally acknowledged.

Associate editor: Jeremy B. Fein

Appendix A. Supplementary material

Supplementary data associated with this article can be found, in the online version, at doi:10.1016/j.gca.2005.10.026.

References

Ahner, B.A., Morel, F.M.M., Moffett, J.W., 1997. Trace metal control of phytochelatin production in coastal waters. *Limnol. Oceanogr.* **42**, 601–608.

Albarede, F., 2004. The stable isotope geochemistry of copper and zinc. In: Johnson, C.M., Beard, B.L., Albarede, F. (Eds.), *Geochemistry of Non-traditional Stable Isotopes*, vol. 55. Mineralogical Society of America, Geochemical Society.

Allison, J.D., Brown, D.S., Novo-Gradac, K.J., 1991. *MINTEQA2/PRODEFA2, A Geochemical Assessment Model for Environmental Systems: Version 3.0 User's Manual*. U.S. EPA, Athens, GA.

Anderson, M.A., Morel, F.M.M., Guillard, R.R.L., 1978. Growth limitation of a coastal diatom by low zinc ion activity. *Nature* **276**, 70–71.

Barling, J., Anbar, A.D., 2004. Molybdenum isotope fractionation during adsorption by manganese oxides. *Earth Planet. Sci. Lett.* **217**, 315–329.

Beveridge, T.J., 1988. The bacterial surface: General consideration towards design and function. *Can. J. Microbiol.* **34**, 363–372.

Beveridge, T.J., Hughes, M.N., Lee, H., Leung, K.T., Poole, R.K., Savvaidis, I., Silver, S., Trevors, J.T., 1997. Metal–microbe interactions: contemporary approaches. *Adv. Microbiol. Physiol.* **38**, 177–243.

Borrok, D., Fein, J.B., Kulpa, Ch.F., 2004. Proton and Cd adsorption onto natural consortia: testing universal adsorption behavior. *Geochim. Cosmochim. Acta* **68**, 3231–3238.

Boyanov, M.I., Kelly, S.D., Kemner, K.M., Bunker, B.A., Fein, J.B., Fowle, D.A., 2003. Adsorption of cadmium to *Bacillus subtilis* bacterial cell walls: A pH-dependent X-ray absorption fine structure spectroscopy study. *Geochim. Cosmochim. Acta* **67**, 3299–3311.

Brand, L.E., Sunda, W.G., Guillard, R.R.L., 1986. Reduction of marine phytoplankton reproduction rates by copper and cadmium. *J. Exp. Mar. Biol. Ecol.* **96**, 225–250.

Cacaly, S., Marechal, C., Juillot, F., Guyot, F., Benedetti, M., 2004. Zn isotopes fractionation upon sorption and precipitation. In: Abstracts of the 13th Annual V.M. Goldschmidt Conference, June 5–11, Copenhagen, Denmark. *Geochim. Cosmochim. Acta Suppl.*, **68/11S**, A366.

Cox, E.H., McLendon, G.L., Morel, F.M.M., Lane, T.W., Prince, R.C., Pickering, I.J., George, G.N., 2000. The active site structure of *Thalassiosira weissflogii* carbonic anhydrase 1. *Biochemistry* **39**, 12128–12130.

Criss, R.E., 1999. *Principles of Stable Isotope Distribution*. Oxford University Press, Oxford.

Crist, R.H., Oberholser, K., Shank, N., Nguyen, M., 1981. Nature of bonding between metallic ions and algal cell walls. *Environ. Sci. Technol.* **15**, 1212–1217.

Csogor, Z., Melgar, D., Schmidt, K., Posten, C., 1999. Production and particle characterization of the frustules of *Cyclotella cryptica* in comparison with siliceous earth. *J. Biotechnol.* **70**, 71–75.

Daughney, C.J., Fein, J.B., 1998. The effect of ionic strength on the adsorption of H^+, Cd^{2+}, Pb^{2+}, and Cu^{2+} by *Bacillus subtillis* and *Bacilluus licheniformis*: A surface complexation model. *J. Colloid Interface Sci.* **198**, 53–77.

Daughney, C.J., Fein, J.B., Yee, N., 1998. A comparison of the thermodynamics of metal adsorption onto two common bacteria. *Chem. Geol.* **144**, 161–176.

Daughney, C.J., Fowle, D.A., Fortin, D.E., 2001. The effect of growth phase on proton and metal adsorption by *Bacillus subtilis*. *Geochim. Cosmochim. Acta* **65**, 1025–1035.

Delolme, C., Hébrad-Labit, C., Spadini, L., Gaudet, J.-P., 2004. Experimental study and modeling of the transfer of zinc in a low reactive sand column in the presence of acetate. *J. Contam. Hydrol.* **70**, 205–224.

Dixit, S.S., Smol, J.P., Kingston, J.C., Charles, D.F., 1992. Diatoms: powerful indicators of environmental change. *Environ. Sci. Technol.* **26**, 23–33.

Elwood, M.J., Hunter, K.A., 1999. Determination of the Zn/Si ratio in diatom opal: a method for the separation, cleaning and dissolution of diatoms. *Marine Chem.* **66**, 149–160.

Fein, J.B., Daughney, C.J., Yee, N., Davis, T.A., 1997. A chemical equilibrium model for metal adsorption onto bacterial surfaces. *Geochim. Cosmochim. Acta* **61**, 3319–3328.

Fein, J.B., Martin, A.M., Wightman, P.G., 2001. Metal adsorption onto bacterial surfaces: Development of a predictive approach. *Geochim. Cosmochim. Acta* **65**, 4267–4273.

Fein, J.B., Boily, J.-F., Yee, N., Gorman-Lewis, D., Turner, B.F., 2005. Potentiometric titrations of *Bacillus subtilis* cells to low pH and a comparison of modeling approaches. *Geochim. Cosmochim. Acta* **69**, 1123–1132.

Fisher, N.S., 1986. On the reactivity of metals for marine phytoplankton. *Limnol. Oceanogr.* **31**, 443–449.

Fisher, N.S., Fabris, J.G., 1982. Complexation of Cu, Zn, and Cd by metabolites excreted from marine diatoms. *Marine Chem.* **11**, 245–255.

Fisher, N.S., Jones, G.L., Nelson, D.M., 1981. Effects of copper and zinc on growth, morphology and metabolism of *Asterionella japonica* (Cleve). *J. Exp. Mar. Biol. Ecol.* **51**, 37–56.

Fowle, D.A., Fein, J.B., 1999. Competitive adsorption of metal cations onto two Gram-positive bacteria: Testing the chemical equilibrium model. *Geochim. Cosmochim. Acta* **63**, 3059–3067.

Fowle, D.A., Fein, J.B., 2000. Experimental measurements of the reversibility of metal–bacteria adsorption reactions. *Chem. Geol.* **168**, 27–36.

Frausto da Silva, J.J., Williams, R.J.P., 2001. *The Biological Chemistry of the Elements*. Oxford University Press, pp. 315–339.

Galy, A., Pokrovsky, O.S., Schott, J., 2002. Ge-isotopic fractionation during its sorption on goethite: an experimental study. In: Abstracts of the V.M. Goldschmidt Conference, August 18–23, Davos, Switzerland. *Geochim. Cosmochim. Acta Suppl.*, **66**, A259.

Gélabert, A., Pokrovsky, O.S., Schott, J., Boudou, A., Feurtet-Mazel, A., Mielczarski, J., Mielczarski, E., Mesmer-Dudons, N., Spalla, O., 2004. Study of diatoms/aqueous solution interface. I. Acid–base equilibria, surface charge and spectroscopic observation of freshwater and marine species. *Geochim. Cosmochim. Acta* **68**, 4039–4058.

Genter, R.B., 1996. Ecotoxicology of inorganic chemical stress to algae. In: Stevenson, R.J., Bothwell, M.L., Lowe, R.L. (Eds.), *Algal Ecology of Freshwater Benthic Ecosystems, Aquatic Ecology Series*. Academic Press, Boston, pp. 404–468.

Gold, C., Feurtet-Mazel, A., Coste, M., Boudou, A., 2002. Field transfer of periphytic diatom communities to assess short-term structural effects of metals (Cd, Zn) in rivers. *Water Res.* **36**, 3654–3664.

Gold, C., Feurtet-Mazel, A., Coste, M., Boudou, A., 2003a. Effect of cadmium stress on periphytic diatom communities in indoor artificial streams. *Freshwater Biol.* **48**, 316–328.

Gold, C., Feurtet-Mazel, A., Coste, M., Boudou, A., 2003b. Impacts of metals (Cd, Zn) on the development of periphytic diatom communities within outdoor artificial streams along a pollution gradient. *Arch. Environ. Toxicol.* **44**, 189–197.

Goncalves, M.L.S., Sigg, L., Reutlinger, M., Stumm, W., 1987. Metal ion binding by biological surfaces: voltametric assessment in the presence of bacteria. *Sci. Total Environ.* **60**, 105–119.

Gonzalez-Davila, M., 1995. The role of phytoplankton cell on the control of heavy metal concentrations in seawater. *Marine Chem.* **48**, 215–236.

Gonzales-Davila, M., Santana-Casiano, J.M., Laglera, L.M., 2000. Copper adsorption in diatom cultures. *Marine Chem.* **70**, 161–170.

Gonzales-Davila, M., Santana-Casiano, J.M., Perez-Pena, J., Millero, F.J., 1995. Binding of Cu(II) to the surface and excudates of the alga *Dunaliela tertiolecta* in seawater. *Environ. Sci. Technol.* **29**, 289–301.

Guiné, V., Spadini, L., Muris, M., Sarret, G., Delolme, C., Gaudet, J.-P., Martins, J.M.F., 2005. Zinc sorption to cell wall components of three Gram-negative bacteria: a combined titration, modeling and EXAFS study. *Environ. Sci. Technol.* (in press).

Gunneriusson, L., Sjoberg, S., 1993. Surface complexation in the H^+-goethite (α-FeOOH)–Hg (II)–chloride system. *J. Colloid Interface Sci.* **156**, 121–128.

Haas, J.R., Dichristina, T.J., Wade Jr., R., 2001. Thermodynamics of U(VI) sorption onto *Shewanella putrefaciens*. *Chem. Geol.* **180**, 33–54.

Hecky, R.E., Mopper, K., Kilham, P., Degens, E.T., 1973. The amino acid and sugar composition of diatom cell-walls. *Marine Biol.* **19**, 323–331.

Herbelin, A.L., Westall, J.C., 1996. FITEQL version 3.2, a computer program for determination of chemical equilibrium constants from experimental data. Department of Chemistry, Oregon State University, Corvallis, OR 97331.

Iller, R.K., 1979. *The Chemistry of Silica*. Wiley, New York, p. 665.

Ivorra, N., Bremer, S., Guasch, H., Kraak, M.H.S., Admiraal, W., 2000. Differences in the sensitivity of benthic microalgae to Zn and Cd regarding biofilm development and exposure history. *Environ. Toxicol. Chem.* **19**, 1332–1339.

Jensen, A., Rystad, B., Melsom, S., 1974. Heavy-metal tolerance of marine phytoplankton. 1. Tolerance of 3 algal species to zinc in coastal seawater. *J. Exp. Mar. Biol. Ecol.* **15**, 145–157.

Jensen, T.E., Baxter, M., Rachlin, W., Jani, V., 1982. Uptake of heavy metals by *Plectonema boryanum* (Cyanophyceae) into cellular components, especially polyphosphate bodies: an X-ray energy dispersive study. *Environ. Pollut. Ser. A* **27**, 119–127.

Johnson, C.M., Beard, B.L., Albarede, F., 2004. Geochemistry of non-traditional stable isotopes. *Min. Soc. Am.* **55**.

Kiefer, E., Sigg, L., Schosseler, P., 1997. Chemical and spectroscopic characterization of algae surfaces. *Environ. Sci. Technol.* **31**, 759–764.

Klimmek, S., Stan, H.-J., Wilke, A., Bunke, G., Buchholz, R., 2001. Comparative analysis of the biosorption of cadmium, lead, nickel, and zinc by algae. *Environ. Sci. Technol.* **35**, 4283–4288.

Kola, H., Wilkinson, K.J., 2005. Cadmium uptake by a green alga can be predicted by equilibrium modeling. *Environ. Sci. Technol.* **39**, 3040–3047.

Kotrba, P., Macek, T., Ruml, T., 1999. Heavy metal-binding peptides and proteins in plants. A review. *Collect. Czech. Chem. Commun.* **64**, 1057–1086.

Lemarchand, E., Schott, J., Gaillardet, J., 2005. Boron isotopic fractionation related to boron sorption on humic acid and the structure of surface complexes formed. *Geochim. Cosmochim. Acta* **69**, 3519–3533.

Lützenkirchen, J., 1999. The constant capacitance model and variable ionic strength: an evaluation of possible applications and applicability. *J. Colloid Interface Sci.* **217**, 8–18.

Maréchal, C.N., Albarède, F., 2002. Ion-exchange fractionation of copper and zinc isotopes. *Geochim. Cosmochim. Acta* **66**, 1499–1509.

Maréchal, C.N., Telouk, P., Albarède, F., 1999. Precise analysis of copper and zinc isotopic compositions by plasma-source mass spectrometry. *Chem. Geol.* **156**, 251–273.

Martell, A.E., Smith, R.M., Motekaitis, R.J., 1997. NIST Critically selected stability constants of metal complexes. Database software version 3.0. Texas A & M University, College Station, TX.

Mirimanoff, N., Wilkinson, K.J., 2000. Regulation of Zn accumulation by a freshwater Gram-positive bacterium (*Rhodococcus opacus*). *Environ. Sci. Technol.* **34**, 616–622.

Morel, F.M.M., Hudson, R.J.M., Price, N.M., 1991. Limitation of productivity by trace metals in the sea. *Limnol. Oceanogr.* **36**, 1742–1755.

Morel, F.M.M., Reinfelder, J.R., Roberts, S.B., Chamberlan, C.P., Lee, J.G., Yee, D., 1994. Zinc and carbon colimitation of marine phytoplankton. *Nature* **269**, 740–742.

Ngwenya, B.T., Suthermand, I.W., Kennedy, L., 2003. Comparison of the acid–base behaviour and metal adsorption characteristics of a Gram-negative bacterium with other strains. *Appl. Geochem.* **18**, 527–538.

Phinney, J.T., Bruland, K.W., 1994. Uptake of lipophilic organic Cu, Cd, and Pb complexes in the coastal diatom *Thalassiosira weissflogii*. *Environ. Sci. Technol.* **28**, 1781–1790.

Pichat, S., Douchet, C., Albarède, F., 2003. Zinc isotope variations in deep-sea carbonates from the eastern equatorial Pacific over the last 175 ka. *Earth Planet. Sci. Lett.* **210**, 167–178.

Plette, A.C.C., Benedetti, M.F., van Riemsdijk, W.H., 1996. Competitive binding of protons, calcium, cadmium, and zinc to isolated cell walls of a Gram-positive soil bacterium. *Environ. Sci. Technol.* **30**, 1902–1910.

Pokrovsky, O.S., Pokrovski, G.S., Gélabert, A., Schott, J., Boudou, A., 2005a. Speciation of Zn associated with diatoms using X-ray absorption spectroscopy. *Environ. Sci. Technol.* **39**, 4490–4498.

Pokrovsky, O.S., Viers, J., Freydier, R., 2005b. Zinc stable isotope fractionation during its adsorption on oxides and hydroxides. *J. Colloid Interface Sci.* **291**, 192–200.

Pun, K.C., Cheung, R.Y.H., Wong, M.H., 1995. Characterization of sewage sludge and toxicity evaluation with microalgae. *Marine Poll. Bull.* **31**, 394–401.

Rijstenbil, J.W., Gerringa, L.J.A., 2002. Interactions of algal ligands, metal complexation and availability, and cell responses of the diatom *Ditylum brightwellii* with a gradual increase in copper. *Aquatic Toxicol.* **56**, 115–131.

Rijstenbil, J.W., Sandee, A., Van Drie, J., Wijnholds, J.A., 1994. Interaction of toxic trace metals and mechanisms of detoxification in the planctonic diatoms *Ditylum brightwellii* and *Thalassiosira pseudonana*. *FEMS Microbiol. Rev.* **14**, 387–396.

Rouseset, D., Henderson, G.M., Shaw, S., 2004. Cu and Zn isotope fractionation during sorption experiments. In: Abstracts of the 13th Annual V.M. Goldschmidt Conference, June 5–11, Copenhagen, Denmark. *Geochim. Cosmochim. Acta Suppl.*, **68/11S**, A360.

Santana-Casiano, J.M., Gonzalez-Davila, M., Perez-Pena, J., Millero, F., 1995. Pb^{2+} interactions with marine phytoplankton *Dunaliela tertiolecta*. *Marine Chem.* **48**, 115–129.

Santana-Casiano, J.M., Gonzalez-Davila, M., Laglera, L.M., Pérez-Pena, J., Brand, L., Millero, F.J., 1997. The influence of zinc, aluminum and cadmium on the uptake kinetics of iron by algae. *Marine Chem.* **59**, 95–111.

Schiewer, S., Volesky, B., 1995. Modeling of the proton–metal ion exchange in biosorption. *Environ. Sci. Technol.* **29**, 3049–3058.

Schmitt, D., Muller, A., Csogor, Z., Frimmel, F.H., Posten, C., 2001. The adsorption kinetics of metal ions onto different microalgae and siliceous earth. *Water Res.* **35**, 779–785.

Slaveykova, V.I., Wilkinson, K.J., 2002. Physicochemical aspects of lead bioaccumulation by *Chlorella vulgaris*. *Environ. Sci. Technol.* **36**, 969–975.

Smiejan, A., Wilkinson, K.J., Rossier, C., 2003. Cd bioaccumulation by a freshwater bacterium, *Rhodospririllum rubrum*. *Environ. Sci. Technol.* **37**, 701–706.

Stauber, J.L., Florence, T.M., 1990. Mechanism of toxicity of zinc to the marine diatom *Nitzschia closterium*. *Marine Biol.* **105**, 519–524.

Sunda, W.G., Huntsman, S.A., 1992. Feedback interactions between zinc and phytoplankton in seawater. *Limnol. Oceanogr.* **37**, 25–40.

Sunda, W.G., Huntsman, S.A., 1998. Processes regulating cellular metal accumulation and physiological effects: Phytoplankton as model systems. *Sci. Total Environ.* **219**, 165–181.

Sverjensky, D., Sahai, N., 1996. Theoretical prediction of single-site surface-protonation equilibrium constants for oxides and silicates in water. *Geochim. Cosmochim. Acta* **60**, 3773–3797.

Tien, C.-J., 2004. Some aspects of water quality in a polluted lowland river in relation to the intracellular chemical levels in planktonic and epilithic diatoms. *Water Res.* **38**, 1779–1790.

Vallee, B.L., Auld, D.S., 1990. Zinc coordination, function, and structure of zinc enzymes and other proteins. *Biochemistry* **29**, 5647–5659.

Viers, J., Oliva, P., Freydier, R., Dupre, B., 2004. The use of Zn isotopes to constrain the biogeochemical cycling of metals in watersheds. *Geochim. Cosmochim. Acta Suppl.* **68**, A413, N11S.

Volesky, B., Holan, Z.R., 1995. Biosorption of heavy metals. *Biotechnol. Prog.* **11**, 235–250.

Vrieling, E.G., Beelen, T.P.M., van Santen, R.A., Gieskes, W.W.C., 2000. Nanoscale uniformity of pore architecture in diatomaceous silica: a combined small and wide angle X-ray scattering study. *J. Phycol.* **36**, 146–159.

Wang, W.-X., Dei, R.C.H., 2001a. Effects of major nutrient additions on metal uptake in phytoplankton. *Environ. Pollut.* **111**, 233–240.

Wang, W.-X., Dei, R.C.H., 2001b. Metal uptake in a coastal diatom influenced by major nutrients (N, P, and Si). *Water Res.* **35**, 315–321.

Webb, S.M., Gaillard, J.-F., Jackson, B.E., Stahl, D.A., 2001. An EXAFS study of zinc coordination in microbial cells. *J. Synchrotron Rad.* **8**, 943–945.

Westall, J.C., Jones, J.D., Gary, D., Turner, G.D., John, M., Zachara, J.M., 1995. Models for association of metal ions with heterogeneous environmental sorbents. 1. Complexation of Co(II) by leonardite humic acid as a function of pH and $NaClO_4$ concentration. *Environ. Sci. Technol.* **29**, 951–959.

Xue, H.-B., Stumm, W., Sigg, L., 1988. The binding of heavy metals to algal surfaces. *Water Res.* **22**, 917–926.

Yee, N., Fein, J., 2001. Cd adsorption onto bacterial surfaces: A universal adsorption edge? *Geochim. Cosmochim. Acta* **65**, 2037–2042.